

Spring 5-15-2017

Apparent retention volume variation with flow rate change in high performance liquid chromatography

Susanne Buntz Erz

Seton Hall University, susanne.erk@gmail.com

Follow this and additional works at: <https://scholarship.shu.edu/dissertations>



Part of the [Analytical Chemistry Commons](#)

Recommended Citation

Erz, Susanne Buntz, "Apparent retention volume variation with flow rate change in high performance liquid chromatography" (2017). *Seton Hall University Dissertations and Theses (ETDs)*. 2282.
<https://scholarship.shu.edu/dissertations/2282>

**Apparent retention volume variation with
flow rate change in high performance liquid
chromatography**

By:

Susanne Buntz Erz

Dissertation submitted to the Department of Chemistry and Biochemistry of
Seton Hall University in partial fulfillment of the requirements for the degree
of

DOCTOR of PHILOSOPHY

in

Chemistry

May 2017

South Orange, New Jersey

© Copyright 2017

Susanne Buntz Erz


All Rights Reserved

We certify that we have read this thesis and that our opinion it is sufficient in scientific scope and quality as a dissertation for the degree of Doctor of Philosophy

APPROVED




Yuri Kazakevich, Ph.D.
Research Adviser



Nicholas H. Snow, Ph.D.
Member of Dissertation Committee



Alexander Fadeev, Ph.D.
Member of Dissertation Committee



Cecilia Marzabadi, Ph.D.
Chair, Department of Chemistry and Biochemistry

This work is dedicated to:

My parents:

Hans and Ursula Buntz

My husband:

Kurt Erz

My children:

Kyle, Jordan and Hanna

Abstract

Recent studies have demonstrated noticeable flow rate dependency of the chromatographic zone retention volume with respect to migration within the empty capillary. This appears to be the result of superposition of asymmetric lateral diffusion and of the laminar flow profile. Although these effects have been studied on empty capillaries, in the presence of the packed column, the retention shift may be insignificant relative to the adsorption-based retention of the analytes. In the case of fast and ultrafast HPLC with short capillary columns, the effect of extra-column caused variation in the analyte retention may constitute an increase of up to 120 % of the overall retardation. Small columns have very small column void volume, e.g. 1.0 x 50 mm with a column void volume of 24 μl , where the extra column volume within the connecting capillary can be as great as 185 μl . This great difference in volume, especially considering that some systems contain even longer connecting tubing for 2 dimensional HPLC or LC-MS systems, can demonstrate a significant shift in the overall retardation and may cause identification and quantitation problems.

Experiments were done with common mobile phase solvents and readily available peek tubing at different variation of length and inner diameter.

The origin of the phenomena is discussed, as well as the main influencing parameters such as capillary material, internal diameter, type and composition of the mobile phase.

This research illustrates the importance of extra column volume on the overall separation in HPLC. The degree of band broadening and the apparent increase in retention volume is driven by the laminar flow profile and concomitant diffusion between the layers within the connective tubing of the HPLC system. The process of molecular diffusion alone has been shown to have negligible impact on this effect and is a positive outcome for systems requiring "parking" within sample loops such as in LC x LC systems. However, the deformation of sample plugs due to laminar flow effects were greatest at higher flow rates and in narrower tubing, which could have a significant impact on fast LC technologies such as UHPLC, short and narrow columns, and systems with unavoidable additional tubing lengths. This effect should be considered during method development and transfers between HPLC systems with variable extra column tubing dimensions and especially when utilizing micro columns with non-porous particles or in cases of minimally retentive analytes.

Acknowledgement

This dissertation would not be possible without the many people in my life supporting me.

I would like to thank my mentor Dr. Yuri Kazakevich for accepting me as a graduate student in his research group and for the years of guidance, patience, and inspiration he has given me. I will miss the time our research group spend in the laboratory working, arguing and laughing.

I would also like to thank Dr. Nicholas Snow for being on my dissertation committee and for the many valuable insights he has given me during my research in the laboratory and in our group meetings.

I would like to thank Dr. Alexander Fadeev on being on my dissertation committee and for sharing his knowledge in physical chemistry.

I would like to acknowledge all the people in the department of Chemistry and Biochemistry for all of their support and assistance during my time at the University.

I would especially like to thank my mother for her continuous support, confidence and encouragement during my time of study as well my father-in-

law Manfred Erz for his support and help with the kids so I could have time to write.

I would also like to thank my sister Hanne Schloemer for her continuous encouragement and confidence in me.

I would very much like to thank my children for being so patient and helpful during my writing period. I know it was not easy on them and I hope that this work will inspire them to pursuit their own passions.

Lastly, I am thankful for my husband Kurt for his tremendous help at home, his constant motivation and trust in me. Without his loving support, completion of this work would not have been possible.

Table of Contents

1.	Introduction	1
1.1	Chromatographic parameters.....	4
1.1.1	Retention volume, column void volume, and extra column volume	4
1.1.2	Efficiency	11
1.2	Flow parameters	15
1.2.1	Reynolds number	16
1.2.2	Newtonian fluids	19
1.2.3	Poiseuille flow	21
1.2.4	Laminar flow	24
1.3	Diffusion and dispersion	30
1.3.1	Diffusion.....	31
1.3.2	Brownian motion by A. Einstein	32
1.3.3	Dispersion.....	35
2.	Scope of the research.....	40
3.	Experimental	42
3.1	Instrumentation and software	42
3.2	Chemicals and material	43
3.3	Environment	43
3.4	Experimental designs.....	44
3.4.1	Extra column volume measurements under normal condition .	44

3.4.2	Extra column measurement under “super slow flow” conditions .	46
3.4.3	Extra column measurement under “stop flow” conditions	47
4.	Results and Discussion.....	50
4.1	Zone marker migration comparison between mobile phases and variation of the flow rate	51
4.2	Variation of inner diameter of PEEK tubing	56
4.3	Stainless Steel Tubing.....	68
4.4	Greater Range	72
4.5	Super Slow Flow	83
4.6	Stop Flow	86
4.5	Diffusion Proposition and Calculation	88
4.5.1	Diffusion.....	88
4.5.2	Flow contribution	96
4.6	Model Application	115
5.	Conclusions	122
6.	References	126

List of Figures

Figure 1: Gaussian band broadening with σ equals the half width at half height of the distribution curve.	13
Figure 2: Laminar flow profile (on the left) vs turbulent flow profile (on the right).	18
Figure 3: Flow between two parallel plates to demonstrate the viscosity of a fluid. Figure adapted from [32,40]	20
Figure 4: Fluid flow in a pipe with a circular cross section and a pressure difference of ΔP applied between the inlet and outlet ends of the pipe with a length of L.	23
Figure 5: Development of the laminar flow profile in a pipe. Illustration adapted from [32,40]	27
Figure 6: Illustration of the instrumental setup for the extra volume measurements. A single piece of tubing was used to connect the injector to the detector without a column.	45
Figure 7: Illustration of the 6-port valve. On the left the switch is on the ON position and on the right side, the switch is on the OFF position ...	49
Figure 8: Comparison of different mobile phases at different flow rates with tubing length of 914.4 mm and ID 0.178 mm. The differences in retention volume between the three different mobile phases are very small when compared to the change of volume caused by the flow rate.	55

Figure 9: Retention volume of deuterated acetonitrile in acetonitrile mobile phase. Comparison of V_R between different inner diameters of the tubing.....	59
Figure 10: Retention volume of deuterated methanol in methanol mobile phase. Comparison of V_R between different inner diameters of the tubing.....	60
Figure 11: Retention volume of deuterated water in water mobile phase. Comparison of V_R between different inner diameters of the tubing	61
Figure 12: Normalized data of measured retention volume and theoretical tubing volume (0.02" = 0.508 mm, 0.01" = 0.254 mm, 0.007" = 0.178 mm).....	64
Figure 13: Retention volume versus flow rate on stainless steel tubing with acetonitrile and water	71
Figure 14: Elution profile comparison of different flow rate from 0.01 ml/min up to 2 ml/min graphed as volume to response on tubing with ID of 0.254 mm.	74
Figure 15: Elution profile comparison of different flow rate from 0.01 ml/min up to 5 ml/min graphed as volume to response on tubing with ID of 0.508 mm.	75
Figure 16: Elution profile graphed in retention volume against response comparison of different flow rates. On the left from 0.5 ml/min to 2 ml/min and on the right side from 0.01 ml/min to 0.1 ml/min. Both on tubing with ID of 0.254 mm.....	77

Figure 17: Elution profile graphed in retention volume against response comparison of different flow rates. On the left from 0.5 ml/min to 5 ml/min and on the right side from 0.01 ml/min to 0.1 ml/min. Both on tubing with ID of 0.508 mm.....	78
Figure 18: Summarization of individual peaks at different flow rate (shown on chart title). Y axis is the response and the x axis the retention time in min.....	80
Figure 19: Illustrates the change of the peak width in relation to the change of the flow rate. The peak width is corrected for the flow rate. This is a clearer demonstration that the peak width increases with the increase of velocity.	81
Figure 20: Measurement of retention volume in dependency of flow rate from 0.001 ml/min to 0.005 ml/min normalized for volume	84
Figure 21: Peak broadening experiment under stop flow conditions showing peaks from three different dwell times in loop. The peaks were corrected for the time delay.	87
Figure 22: Idea of diffusion of sample plug in PEEK tubing	90
Figure 23: Comparison of measured and predicted peak width, demonstrating that the measured results are the opposite of what was expected.	95
Figure 24: Diffusion from the inner layer outwards is more favorable than the diffusion form the outer layer inwards.....	101
Figure 25: Concentration gradient from the parabolic flow profile towards the tubing wall, where the concentration on the peripheral layer towards the tubing wall is presumed to be higher.	102

Figure 26: Diffusion direction of the sample plug. The molecules diffuse outward (red arrows) from a higher velocity and concentration into a layer with a lower concentration and slower velocity, whereas the blue arrows demonstrate the direction of the diffusion from the outside layers exhibiting slower velocity into the layer with higher velocity and concentration. 103

Figure 27: Experimental peak width compared to the Taylor equation for the dispersion coefficient K 107

Figure 28: Suggestion of the deformation of the initial sample plug travelling through the capillary 109

Figure 29: Illustrates the parabolic flow profile of the 3 tubings with different size inner diameters. The limit of the x axis is the limit of the length of the capillary and the limit of the y axis is the limit of the radius of the biggest capillary (ID 0.508 mm). 112

Figure 30: Illustrates the last 10% of the capillary length based on the parabolic flow profile. 113

Figure 31: Illustrates the last 5% of the capillary length. The difference in the distance of the outside and inside parabola is increasing by decreasing the capillary ID. 114

Figure 32: Effect of extra column volume on analyte retention on a column with dimensions of 4.6 x 150 mm. 119

Figure 33: Effect of extra column volume on analyte retention on a column with dimensions of 2 x 50 mm 120

Figure 34: Effect of extra column volume on analyte retention on a column with dimensions of 1 x 50 mm 121

List of Tables

Table 1: Retention volume of deuterated acetonitrile in 100 % acetonitrile mobile phase at various flow rates. An increase of the retention volume of 31 μ l has been recorded when the retention volume was measured from the lowest flowrate to the highest flowrate and then compared.....	52
Table 2: Retention volume of deuterated water in 100% water mobile phase at various flow rates. An increase of the retention volume of 39 μ l has been recorded when the retention volume was measured from the lowest flowrate to the highest flowrate and then compared.	53
Table 3: Retention volume of deuterated methanol in 100% methanol mobile phase at various flow rates. An increase of the retention volume of 40 μ l has been recorded when the retention volume was measured from the lowest flowrate to the highest flowrate and then compared.	54
Table 4: Variation of tubing ID with the retention volume measured at different flow rates of different mobile phases. Data displayed is the average retention volume of triplicate measurements.	58
Table 5: Normalized data of the measured retention volume against the actual tubing volume	63
Table 6: Approximation for the retention volume on tubing with ID of 0.127 mm. The values are the averages of the three different	

mobile phases from the previous experiment variation of tubing ID using the equation displayed on the graphs.....	66
Table 7: Increase of the apparent retention volume as percentage in dependency of the flow rate. The trend is more pronounced in tubing with smaller ID	67
Table 8: Summarizes the data of retention volume measurements at different flow rate conditions with acetonitrile on stainless steel HPLC connecting tubing.	69
Table 9: Summarizes the data of retention volume measurements at different flow rate conditions with water on stainless steel HPLC connecting tubing.....	70
Table 10: Measured and calculated value for peak width dependency on flow rate	82
Table 11: Measured and calculated value for peak width dependency on velocity.....	85
Table 12: Summarization of peak width values from measurements and predictions based on calculation of molecular diffusion. The last row in the table demonstrates the hypothetical value of the sample plug width.	93
Table 13: Reynolds number for different mobile phases, flow rate and tubing sizes.....	97

Table 14: Shows the time needed of the flow to develop a laminar flow profile based on equation (14). The dwell time is the time needed for the fluid to travel the entire length of the capillary. 98

Table 15: Calculation based on equation (25) to see if the conditions are greater than 6.9. The data below confirm that to be true. Therefore, axial diffusion in future calculation can be neglected. 105

Table 16: Overview of different column dimensions and the resulting ratio of the column void in comparison to the extra column volume of 31 μ l 118

1. Introduction

High Performance Liquid Chromatography (HPLC) is frequently used in diverse chemistry disciplines to separate, identify, and quantify compounds. Over the years, HPLC has played an essential role in laboratories worldwide. Since the early emergence of HPLC around 1970 [1,2] countless improvements and advancements have been achieved with respect to the instrument, the column, and the understanding of the separation science itself. Professor Horvath pioneered the development of the instrument in which a continuous flow of the liquid phase through a column packed with small glass beads was made possible [3]. This was a great achievement considering the resulting backpressure of the liquid and the robustly sealed plumbing system required. The glass beads employed at that time were spherical solid-core glass beads coated with a porous solid [2,3] and have since been considered as a breakthrough in column technology [4].

The continuous pursuit of developing a better HPLC system has resulted in a multitude of HPLC instrumentation with various detectors [5] and a vast selection of specialty columns for selectively different separation mechanisms [2,4]. Evidently, after examination of almost 50 years of HPLC development, the trend is proceeding towards miniaturization [6,7] in all aspects of its physical properties. The emergence of the so-called ultra-high pressure liquid chromatography (UHPLC) is one indication of the evolution of the new generation of HPLC system. An UHPLC system is capable of an overall

operating pressure of up to around 20,000psi [8]; therefore it is an ideal candidate for a shorter column and smaller inner diameter (ID) packed with particles of 2 μm and smaller. Since the main objective of this UHPLC is a faster analysis time [9–11], without sacrificing the quality of the analysis, the resulting objective in developing shorter and smaller column packed with continuously smaller particles does not come as a surprise. Furthermore, shorter analysis time and smaller column decreases the amount of the mobile phase needed for the analysis which leads to a “greener” and economically more efficient approach to HPLC separation [8,10].

Reduction in the geometrical properties of the column does not necessarily mean reduction in all HPLC instrument properties, e.g. the detector flow cell or the connecting tubing, therefore it would be reasonable to suggest that the ratio of column void volume (V_0) and extra column void volume (V_{ex}) will change as a result the overall column size reduction. It is further reasonable to predict that this change in ratio could cause an inferior overall performance of the chromatographic separation.

Extra column volume (V_{ex}) is a prevalent source for resolution and efficiency loss in modern HPLC system [12–14]. This effect is generally more pronounced for early eluting components [13] and is of main concern in fast LC and multidimensional LC. Consequently, in the aspect of miniaturization, the efficiency loss caused by extra column volume becomes very important.

Column void volume (V_0) is the most critical parameter for any HPLC application, whether it is a simple analytical separation or a complex physical-

chemical study of the separation process. For appropriate characterization of separation a reliable column void volume cannot be calculated without an actual measurement [15–17]. During such an experiment to determine the column void volume, it was observed that the column void volume apparently increases by increasing the flowrate of the mobile phase in the LC system. This phenomenon was investigated to isolate the origin and ascertain the cause of the observed effect. This was critical to identify because even a nominal fluctuation of the column void volume is unacceptable for the purposes of appropriate modelling of separation science. Different approaches and theories were examined to evaluate this effect to further determine the extent of possible contribution it may have to the separation quality in HPLC.

This work continued with the study of the cause of spreading of the sample in the chromatographic zone and discusses the different variances within the process of band broadening while considering extra column volume along with the theories of diffusion and dispersion of a sample within the flow profile. Furthermore, we were interested in determining if this phenomenon could be isolated or had an additive effect with other contributing factors. We hypothesized that it may have a difficult to predict synergetic effect. For this reason, this research focused on open capillaries without a HPLC column. The findings in these studies revealed the importance of an understanding of the extra column effect in order to gain consistent separation performance and a better interpretation of retention mechanism in liquid chromatographic systems.

1.1 Chromatographic parameters

1.1.1 Retention volume, column void volume, and extra column volume

An accurate definition and measurement of the void volume V_0 of a column in liquid chromatography is essential for the correct evaluation of capacity factors. The definition of the column void volume in liquid chromatography has been debated for a long time. There are numerous publications [15–19] about defining and measuring the void volume, however, a suitable experimental determination and unified definition of the void volume has not yet been fully achieved. The consequences already start with the terminology itself. It has been called column hold-up volume (V_m), column void (V_0), and others have termed it column dead volume. This inharmoniousness has caused confusion, since some refer to column dead volume as the total volume of all eluent components within the column bed [15] and others define dead volume as the volume caused by the distance between the tip of a ferrule and the tip of the tubing during an incorrect installation of the column end fittings [20].

In an early dictionary of chromatography the dead volume was defined as the volume between the effective injection point and the effective detection point after deducting the column volume [21], which is confusing since this volume currently is more commonly termed as the extra column volume. The different ways in referring to the column void volume also extend to the

different methods applied in determining the column void volume. The main differences are usually separated roughly into two categories, one the static measurement and the other a dynamic way of measurement [16,17].

J. C. Giddings defined the void volume in his book Unified Separation Science [22] as the following: "For a non-retained peak, traveling entirely in the mobile phase, it is necessary to disgorge all the mobile phase, occupying volume V_m in the column, to bring the peak from the beginning to the end of the column" [22].

The discrepancy in the definition of the void volume comes from the different points of view regarding this subject. Giddings [22] originated his equation based on the theory of zone migration. He uses R as a measure of the retardation of the zone with respect of the mobile phase velocity. Therefore, he stated that if a peak that "experiences no retardation because its solute does not partition into the stationary phase ($R = 1$) is termed a non-retained peak or void peak; such a peak travels at mobile phase velocity v "

$$t_0 = \frac{L}{v} \quad (1)$$

Where t_0 is the "retention" time on the non-retained peak, L = the length of the column and v = the mobile phase velocity. However, this model considers the volume from the point of injection until the detector cell.

Knox and Kaliszan [15] for example assigned the column void volume as a thermodynamic dead-volume V_m and they proposed to define V_m as "the total

volume of all eluent components within the column bed". It is shown that V_m , so defined, is given by [15]:

$$V_m = V_A^* x_A + V_B^* x_B + \dots \quad (2)$$

Where V_A^* etc. are the elution volumes of isotopically labeled eluent components A etc., and x_A etc. are the volume fraction of A etc. in the eluent fed to the column.

Gritti, Kazakevich and Guiochon [16] proposed a "general definition of V_m that is valid in RPLC and that would be independent of the experimental method used to measure it". They define the hold-up volume for a C_{18} column as the difference between the volume of the empty column tube and that of the absorbent. In their paper, they compare the results of experimental methods (pycnometry and minor disturbance method) and discuss the systematic differences observed due to the use of different experimental conditions. They also opposed the definition proposed by Knox since it did not take the nature of the solvent into account (eluent accessibility into small pores; adsorption dependency of eluent composition; and the specific volume dependency on temperature and pressure) [16]. The review paper from C. Rimmer, C. Simmons and J. Dorsey also addresses the need of an unambiguous definition of the void volume in reversed-phase liquid chromatography [17].

In this research the column void volume (V_0) is defined as the volume of the liquid phase within the column and can be converted from the void time (t_0) and the mobile phase flow rate (F) [1].

$$t_0 = F * V_0 \quad (3)$$

The void time can be interpreted as part of the total analyte retention time that the analyte actually spends in the mobile phase moving through the column without retaining on the stationary surface of the column [1]. The method used for determination of the column void volume was similar to the minor disturbance method. The disturbance method [15–17] utilizes the injection of a sample of a deuterated eluent in a single component mobile phase using a refractive index detector. This method is a fast and easy way to get a reliable column void volume measurement when using only one eluent component in the mobile phase.

The definition of retention volume on the other hand is less controvertible. Giddings [22] defined the retention time as “the retention time t_r , is the time needed for the center of the peak to migrate to the end of the column at distance L ”:

$$t_r = \frac{L}{V} = \frac{L}{Rv} \quad (4)$$

Where t_r is the retention time, V is the peak velocity, v is the cross sectional average velocity.

"The retention volume V_r , is the volume of the mobile phase, measured as it emerges at the outlet, necessary to flush the peak center to the end of the column" [22].

It is sufficient to say that the retention volume (V_r) is the product of the retention time (t_r) of the analyte and the mobile phase flow rate. The retention time of the analyte is representative of the distance from the injection point to the elution of the of the peak maxima at the detector at a given flow rate and serves as the identifier for the given analyte on that particular system [1]. Since the retention volume is the product of retention time and mobile phase flow rate, the retention volume is independent of the flow properties.

By obtaining both volumes and times (retention and column void) it is possible to determine the retention factor or capacity factor k [1,20,23].

$$k = \frac{V_r - V_0}{V_0} = \frac{V'_r}{V_0} = \frac{t_r - t_0}{t_0} \quad (5)$$

Where V_r is the retention volume of the analyte, V_0 the column void volume, t_r the retention time of the analyte, t_0 the void time and V'_r is the reduced retention volume, which is the difference between the retention volume and the void volume.

The retention factor is dimensionless and independent on the mobile phase flow rate and column dimensions [1].

When a sample is analyzed in HPLC, the sample is injected and the mobile phase carries the analyte into the tubing, which is connected from the injector outlet to the "front" end of the column. After the analyte passes through the column, the analyte again is transported by the mobile phase through another section of tubing, which is connected from the "end" of the column to the detector inlet. The overall volume contributed by these connecting tubing and the flow cell within the detector is called the extra column volume (V_{ex}). It is the volume external to the column without considering the column void volume.

Usually, the extra column volume is not defined separately, since the extra column volume of a HPLC system does not change under normal circumstances. By measuring the void volume of the column and the retention volume, the extra column volume is automatically integrated into the measured value, since it is not feasible to measure the retention volume of the column without the connecting tubing. With the assumption that the extra column volume does not change, it does not make any difference whether the extra column volume is determined by itself or if the measured column void volume is actually the void volume additional to the extra column volume. The same scenario also applies to the retention volume. The capacity factor therefore would be the same. Unfortunately, the contributing effect of the extra column volume is not so much about the increase of the overall volume, but more so, because it causes band broadening of the

sample; which contributes to the loss in efficiency (Figure 1). Because of this, it is advisable to determine the extra column volume to better account for any extra column effects. Especially in the case of changing from one system to another system, the separation profile can change even if the identical column were to be used. Each system has its own characteristic extra column volume unless certain components of the system changes, e.g. replacement of connecting capillaries.

There are two ways to determine the extra column volume; the first is by calculation, where the volumes of the tubing and the detector flow cell are calculated and added together. The second method is to measure the extra column volume by experimentation. The method is often the same as what would be used for the column void volume determination, where the sample is the deuterated eluent with the "retention" being the time of the deuterated peak elution by refractive index detector.

Greater extra column volume causes loss in resolution and efficiency, which is often referred as the extra column effect. The theory is that during the transport of the analytes through the tubing, it will be subject to a broadening of the band due to differences in the migration velocity of the flow in the tubing between the wall and the center of the tubing [20]. Discussion about the topic of the extra column effect, extra column dispersion, or extra column band broadening has been ongoing for decades. As it is with the subject of column void volume, there are many ways to explain this effect. More in depth explanation can be found in the next chapter.

1.1.2 Efficiency

In liquid chromatography, many properties are related to each other and it is difficult to single out one effect. Efficiency and extra column volume have a strong interconnection with one another. Efficiency is defined as the degree of band broadening of the analyte zone moving through the column. As the analyte travels through the column the sample zone will broaden [1].

It is usually calculated using the following equation:

$$N = 16 \left(\frac{t_r}{w} \right)^2 \quad (6)$$

Where N is the number of theoretical plates; t_r = the retention time on the analyte and w = the peak width at the base. One opinion is, as stated previously, that when the analyte travels through the tubing before entering the column, the sample zone will broaden due the different velocities within the tubing. In other words, the peak width can increase and therefore N will be decreased. Consequently, the extra column effect in a chromatographic system becomes a very important subject. There are multiple ways to approach the topic of band broadening. Before getting into details of the different approaches, an overall statement can be made, which is that extra column volume can cause loss in efficiency. Authors in the past have discussed the spreading of sample peaks in chromatographic systems and how to account for it in the data evaluation [24–26]. An early example by Giddings, described one of the effects of zone spreading as follows: “Zone

spreading will occur in every part of the chromatographic system; from the beginning point to the point of detection” and “As a practical matter it is always advisable to reduce extra-column contributions to zone spreading as much as possible. Such contributions serve only to destroy resolution.” [27].

There are different well-established models that describe band broadening [28–30]. One way is to define extra column band broadening by applying the theory of the second statistical moment of the Gaussian distribution function [22]. This theory can give value to band broadening in the form of variances derived from the normal distribution curve of a sample elution peak.

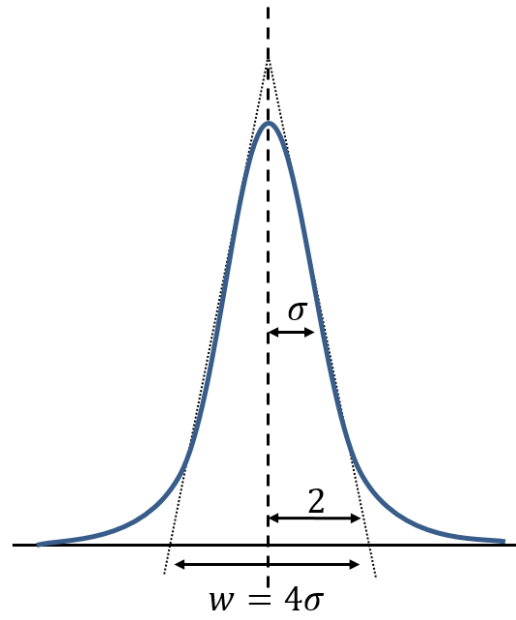


Figure 1: Gaussian band broadening with σ equals the half width at half height of the distribution curve.

Different processes such as molecular diffusion, secondary equilibria, multipath effect, and others contribute their own degree of variance toward the overall band broadening process [1].

$$\sigma_{tot}^2 = \sum \sigma_i^2 \quad (7)$$

The overall band spreading (variance) (σ_{tot}^2) is equal to the sum of the variances (σ_i^2) for each process were each process is assumed to be independent [1].

It can further be described as:

$$\sigma_{tot}^2 = \sigma_{tub}^2 + \sigma_{col}^2 + \sigma_{inj}^2 + \sigma_{det}^2 + \sigma_{other}^2 \quad (8)$$

Where σ_{tot}^2 is the observed peak variance, σ_{tub}^2 the variance originating from the connecting tubing, σ_{col}^2 the variance of the column, σ_{inj}^2 the injector variance, σ_{det}^2 the variance originating from the detector and σ_{other}^2 variance contributions from other processes. By examination of these, it is clear that by increasing the external column volume, the independent variance of $\sum \sigma_i^2$ which is equal to σ_{tot}^2 will be transferred to the equation [31] $w = 4 \sigma$.

1.2 Flow parameters

In HPLC the mobile phase consists of a liquid eluent in contrast to gas chromatography where the mobile phase is in a gaseous phase. Therefore, it is advantageous to explore the subject of fluid dynamics when examining the fundamental characteristics of liquid chromatography.

Generally speaking, dynamics is the study of motion of matter, which can be separated into two parts, the dynamics of rigid bodies and the dynamics of nonrigid bodies [32]. Nonrigid bodies can be generally classified in elasticity (solid elastic bodies) and fluid mechanics. Additionally, the term fluid is classified in two categories, as liquids or gases [32].

This study of the flow of the mobile phase in HPLC, the interest is in the fluid mechanics of the flow of fluids in pipes and channels. Therefore, the focus is in the so-called internal flow where the fluid is usually confined by walls [32]. It is important to consider a steady fluid flow, which is unidirectional in an open tubing/capillary with a constant circular cross section. Gravitational forces are assumed negligible and a steady pressure difference is applied between inlet and outlet ends of the capillary [22].

Flow profiles within a pipe are divided into three different sections. The first is laminar flow, the second is transitional flow, and the third is turbulent flow (see Figure 2). The transitional flow is the region, in which the flow turns from laminar flow profile into turbulent flow profile, and vice versa. The

different flow profiles are calculated and identified using the Reynolds number [33].

1.2.1 Reynolds number

Reynolds number (Re) is a dimensionless quantity used in fluid mechanics to predict the different flow conditions. It is a measure of the ratio of the inertia to viscous force [32]. At a low Reynolds number, the viscous forces are dominant and laminar flow occurs. It is characterized by smooth and constant flow motion. A higher Reynolds number represents a turbulent flow. Turbulent flow is dominated by inertial forces, which are characterized by irregular conditions of the flow in which quantities (e.g. velocity and pressure) show random variation [33]. Under the condition of a flow in a pipe and a Newtonian fluid, the Reynolds number can be defined as [34–37]:

$$Re = \frac{\rho VL}{\mu} = \frac{\rho VD}{\mu} = \frac{VL}{\nu} = \frac{QL}{\nu A} \quad (9)$$

where; ρ = density of fluid, V = mean velocity of fluid, L = characteristic length, D = pipe diameter, μ = dynamic viscosity of fluid, ν = kinematic viscosity, Q = volumetric flow rate, A = cross-sectional area of the tubing. Usually if the Re is smaller than 2000 the flow is considered laminar; if on the other hand, the Re is greater than 4000, the flow is considered turbulent. The region between 2000 and 4000 is considered as the critical or transitional

region of the flow [35,38–40]. Figure 2 illustrates the differences between fluids which have a laminar flow profile and turbulent flow profile in a capillary or tube.

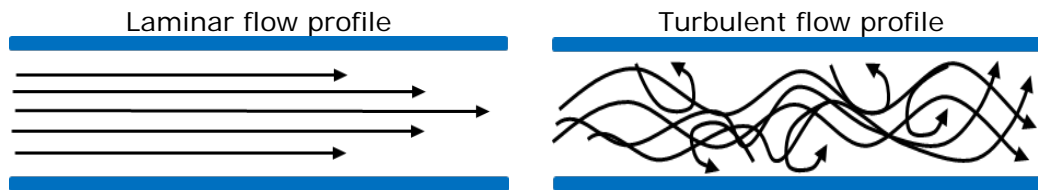


Figure 2: Laminar flow profile (on the left) vs turbulent flow profile (on the right).

1.2.2 Newtonian fluids

All fluids have a defined viscosity which is a measure of the fluid's resistance to shear when the fluid is in motion. A common example to express viscosity (η) is the model in which two plates are parallel to each other and their velocities are linear from zero at the bottom of the plate to U on top of the plate. The fluid between the plates exhibits a linear velocity and at the interface between the fluid and solid, the velocity of the fluid is the same as the solid [32]. The resulting velocity difference causes the fluid to experience stress to overcome the friction between particle layers. These forces are proportional to the area A (the contact area between the plate and the fluid) and the shear rate $\partial v/\partial y$, which can be interpreted as the difference of the velocity Δv of the adjacent layers divided by the distance Δy between these layers [22]. Figure 3 illustrates the flow between two parallel plates to demonstrate the viscosity of a fluid and the forces acting on the fluid flow.

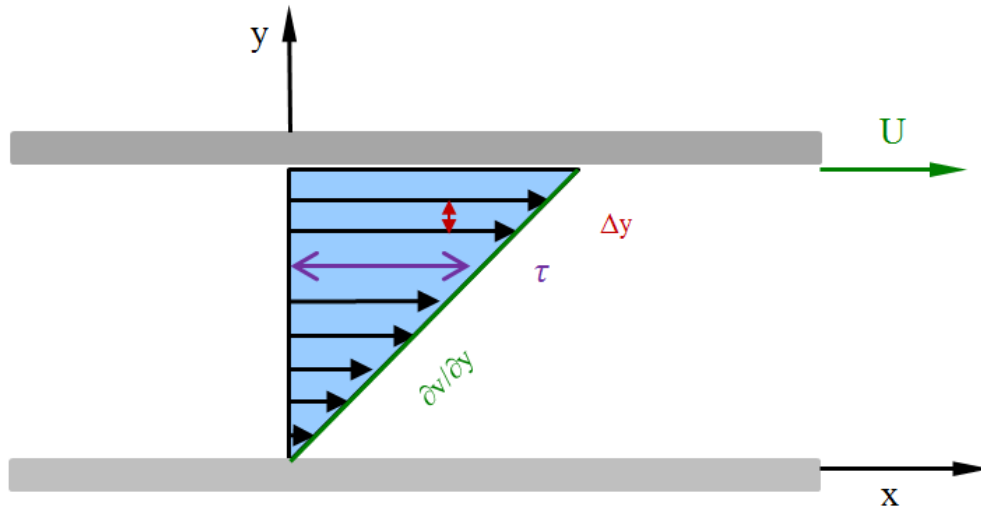


Figure 3: Flow between two parallel plates to demonstrate the viscosity of a fluid. Figure adapted from [32,40].

The shear stress τ acting on the moving layers as illustrated in Figure 3 can be written as:

$$\tau = \eta \frac{\partial v}{\partial y} \quad (10)$$

Where η is the dynamic viscosity, v the velocity, and y the distance.

The viscous force F_η can be expressed as [22]:

$$F_\eta = \eta A \frac{\partial v}{\partial y} \quad (11)$$

From this equation, it can be seen that the greater the viscosity the greater force resisting the shear motion. The viscosity of liquid is strongly dependent on the temperature and very little on pressure in comparison. If the fluid expresses a linear relationship between shear stress and shear rate (velocity gradient), it is considered a Newtonian fluid.

1.2.3 Poiseuille flow

A Poiseuille flow is a pressure-induced flow usually in a pipe with a steady pressure difference ΔP applied between the inlet and outlet ends of the pipe [41]. It is distinguished from drag-induced flow such as Couette Flow [32].

The Poiseuille flow is assumed to exhibit a fully-developed laminar flow profile with an incompressible Newtonian fluid ($P = \text{constant}$) of viscosity μ [32]. Furthermore, it is unidirectional (purely axial direction where the radial velocity is equal to the angular velocity which is zero $v_r = v_\theta = 0$) and its geometry is that of a circular cylindrical pipe with a length L and a radius r . This flow geometry is analyzed using cylindrical polar coordinates (r, θ, z) with the origin on the center line of the pipe entrance and z -direction aligned with the center line [42]. It is assumed that the flow is at a steady state ($\partial/\partial t = 0$) with axisymmetric ($\partial/\partial \theta = 0$) and that there are no gravitational and acceleration forces at play. Therefore, the resulting balance is pressure acting against viscous forces [22]. Figure 4 depicts the circumstance of Poiseuille flow in a pipe with a circular cross section.

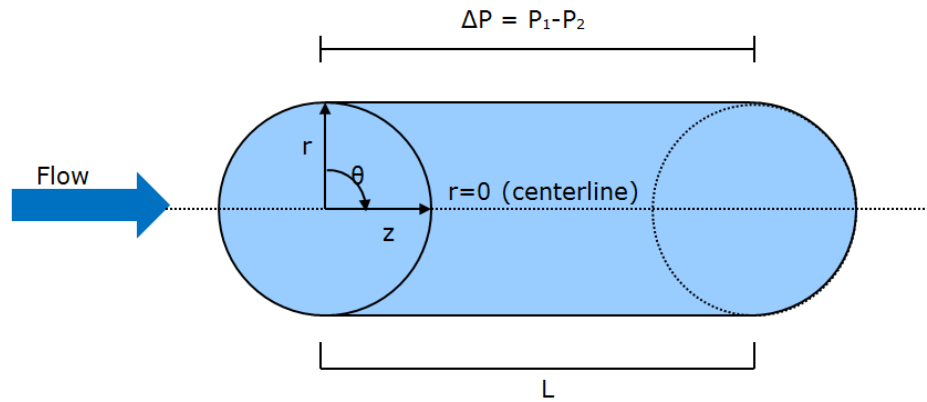


Figure 4: Fluid flow in a pipe with a circular cross section and a pressure difference of ΔP applied between the inlet and outlet ends of the pipe with a length of L .

The more common equation to express Poiseuille flow is the use of the Hagen-Poiseuille equation or Poiseuille's law [41,43,44]:

$$Q = \frac{\pi D^4 P}{128 \mu L} \quad (12)$$

or

$$\Delta P = \frac{8 \mu L Q}{\pi r^4} \quad (13)$$

Where Q is the volumetric flow rate, D is the pipe diameter, π the mathematical constant pi, P the pressure difference along the pipe, μ the dynamic viscosity of the fluid, r the radius of the pipe and L the length of the pipe, which is the distance between the inlet and outlet pressure of the pipe.

1.2.4 *Laminar flow*

When fluid enters a pipe with a circular cross section, at a constant velocity, and a low Reynolds number ($Re < 2000$), it develops a laminar flow profile. Laminar flow is a highly-ordered fluid motion characterized by smooth layers of fluid. Those layers of fluid are called laminar [40]. It is assumed that the layer closest on the wall (surface of the inner tubing) will exhibit zero velocity and the layer at the center the maximum velocity with a symmetrical velocity distribution about the y axis [32,40,45]. After the entrance region, the flow develops from a flat profile all the way to a parabolic profile [46] (see

illustration in Figure 5). The reason for this deformation [47] of the initial flat flow profile is that the layer which comes in contact with the inner pipe wall will have a zero velocity moment caused by the so called no-slip condition. This layer will then slow down the adjacent fluid layer as a result of viscous forces between the next layer and will cascade to each subsequent layer toward the center of the tubing. To compensate for the velocity reduction, the velocity at the center of the pipe will increase in order to keep the mass flow rate through the pipe constant. The flow region adjacent to the inner wall is called the boundary layer where the viscous and frictional effects are significant [32,40]. The region in the center, the so called irrotational flow region, will exhibit insignificant friction forces and the velocity remains constant in the radial direction [40]. Those assumption are necessary in order to establish equations to predict velocity as a function of position in fully developed flow [48].

As shown graphically in Figure 5, the starting position is at point (I). At this point, the flow velocity remains constant in the radial direction giving the average velocity V_{avg} equal to the maximum velocity V_{max} . Point (II) demonstrates the effect of the no-slip condition at the wall, causing the layer adjacent to the wall to slow down towards zero velocity. The boundary layer (depicted with yellow lines) increases and the flow profile exhibits different velocities. At point (III) to point (IV) the boundary layer almost fills the entire pipe. The center of the pipe increases in velocity and the velocity directly at the wall is zero. Point (V) illustrates the fully developed laminar flow profile. The parabolic flow profile is the result of the different velocities

within the flow. At this point, the flow is considered steady and fully developed meaning that there is no change in velocity or other properties, and the shear stress τ_w remains constant as well.

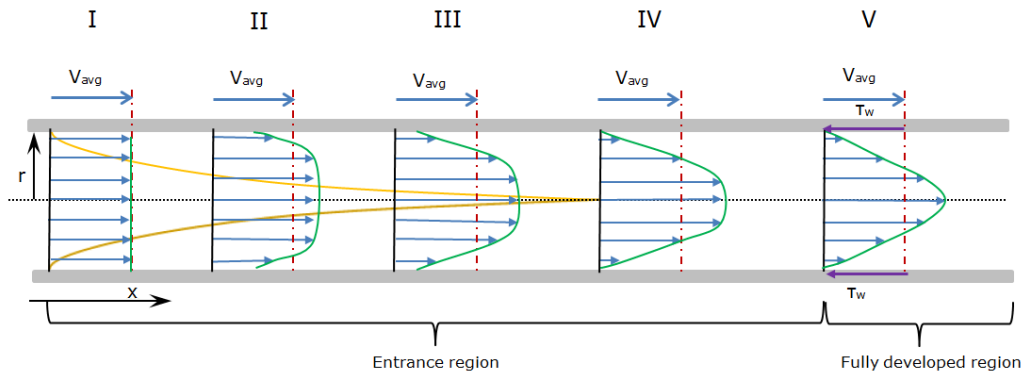


Figure 5: Development of the laminar flow profile in a pipe. Illustration adapted from [32,40].

The entrance length is the point on which the fluid is entering a pipe until it reaches the fully developed flow profile. In the case of laminar flow in a pipe with a circular cross section, the entrance length can be estimated with the following equation [40,49]:

$$L_{h_{laminar}} \approx 0.06 * Re * D \quad (14)$$

Where $L_{h, laminar}$ is the entrance length, Re the Reynolds number, and D is the diameter of the tubing.

The velocity profile of a laminar, incompressible, steady flow with constant properties in the fully developed region of a straight pipe with a circular cross section, where the entrance effects are negligible [40] can be expressed in an equation (see equation 15). It is also assumed that each fluid particle moves at a constant axial velocity and the velocity profile is unchanged, and that there is not motion in the radial direction [40].

The velocity profile $u(r)$ can be determined by applying certain boundary conditions [40]. Using the boundary condition illustrated in Figure 3 and applying it to a circular pipe as illustrated in Figure 4, the boundary condition can be set as follow: $u = 0$ at $r = R$. This condition shows that there is zero velocity at the wall where r (radius of the volume element) is equal to R (the radius of the pipe). Furthermore, $\partial u / \partial r = 0$ at $r = 0$; the velocity over the distance of the volume element is zero at the centerline (where $r = 0$). Note

that the case here is a circular pipe, consequently the above expression changed from ∂y (distance between plates as stated in Figure 3) to ∂r (distance between circular layers expressed as radius).

$$u(r) = -\frac{R^2}{4\mu} \left(\frac{\partial P}{\partial x} \right) \left(1 - \frac{r^2}{R^2} \right) \quad (15)$$

Where R is the radius of the tubing, $\partial P/\partial x$ is the partial differential of the pressure acting on the length of the fluid layer, and r is the radius of that volume element. In this equation above, the values of μ , $\partial P/\partial x$ and R are constant, which means that the velocity (u) varies with the square of r . This in turn shows that the velocity distribution across the section of the tubing is parabolic in nature with a maximum velocity at the centerline and a zero velocity at the tubing wall [50].

The average velocity is expressed as follows [40]:

$$v_{avg} = \frac{2}{R^2} \int_0^R u(r) r \partial r \quad (16)$$

And can be further expressed by substituting the velocity profile from equation (14) into equation (15)

$$v_{avg} = \frac{-2}{R^2} \int_0^R \frac{R^2}{4\mu} \left(\frac{\partial P}{\partial x} \right) \left(1 - \frac{r^2}{R^2} \right) r dr \quad (17)$$

∴

$$v_{avg} = -\frac{R^2}{8\mu} \left(\frac{\partial P}{\partial x} \right) \quad (18)$$

By combining the equations of $u(r)$ and v_{avg} the equation can therefore be written as [36,51,52]:

$$u(r) = 2v_{avg} \left(1 - \frac{r^2}{R^2} \right) \quad (19)$$

The velocity is at maximum when $r = 0$. By substituting $r = 0$ into the previous equation the maximum velocity $u(r)$ can be expressed as [40,50,53]:

$$u_{max} = 2v_{avg} \quad (20)$$

This equation shows that the maximum velocity (in the center of the tubing) is two times higher than the average velocity in the tubing.

1.3 Diffusion and dispersion

Molecule displacements in liquid chromatography are generally the result of diffusion, sorption kinetics, and flow [27]. Sorption kinetics in HPLC primarily takes place within the column which is not the focus in this research; therefore, sorption kinetics will be neglected for the purposes of this research.

Displacement caused by flow and diffusion will be closer investigated to gain a better understanding of the dispersion behavior of the analyte molecule flowing within the solvent stream.

1.3.1 Diffusion

Diffusion is caused by random molecular motion that leads to complete mixing [54]. Based on Fick's first law, it is driven by the concentration gradient, where atoms or molecules from a higher concentration region move to a region of a lower concentration [54]. This one dimensional diffusion equation is expressed as the flux of particles through a unit measure per unit time follow [55,56]:

$$J = -D \frac{\partial c}{\partial x} \quad (21)$$

Where J is the diffusion flux, D is the diffusion coefficient, and $\partial c/\partial x$ is the concentration gradient of the amount x of substance per unit volume to the position x in length [22]. The quantity J will equal the number of moles passing through a unit area in unit time [27].

For radial diffusion in cylindrical coordinates, Fick's law of diffusion without convection can be expressed as follows [54]:

$$-J = D \frac{\partial c}{\partial r} \quad (22)$$

Molecular diffusion flux is more prevalent in laminar flow than in turbulent flow. The diffusion takes place between the laminar layers where the molecules flow along the flow direction within the lamina layer and with different velocities relative to another lamina. This creates concentration gradient perpendicular to the flow direction causing the diffusion across streamlines. Whereas during turbulent flow, the rather chaotic flow profile causes an intense mixing, creating eddies that transport the molecules much more rapidly within the different flow profiles, overshadowing the effect of molecular diffusion [40].

1.3.2 Brownian motion by A. Einstein

Brownian motion is named after the botanist Robert Brown who qualified the random walk of microscopic particles [57]. The random walk model is a one-dimensional random process in which molecular displacements occur [27]. The direction of the "walk" of the molecule is entirely by chance. The mathematical form of Brownian motion was derived by Albert Einstein and published in his paper in 1905 [58]. He stated that : "Evidently it must be assumed that each single particle executes a movement which is independent of the movement of all other particles; the movement of one and the same particle after different intervals of time must be considered as mutually

independent process, ..." [58]. The following equation expresses the mean square displacement in terms of the time elapsed and the diffusivity [53,58,59]:

$$\lambda_x = \sqrt{x^2} = \sqrt{2Dt} \quad (23)$$

Where λ_x is the displacement of the particle in the direction of the x axis in time, D is the diffusion coefficient adapted from Fick, and t is the time.

Giddings [27] used Einstein's equation for a simple treatment of ordinary molecular diffusion as one of the sources of zone spreading (band broadening) [27,36]:

$$\sigma^2 = 2Dt_D \quad (24)$$

This equation is built on the theory of the Gaussian distribution function in particular of the second moment, called the variance σ^2 [22]. The square root of σ is called the standard deviation and is a measure of the overall width of the zone and therefore for the Gaussian zones, σ is the distance from the zone center to the point of inflection [22].

For a zone in uniform translation at constant velocity W , the distance X traversed by the zone in time t is [22]:

$$X = Wt \quad (25)$$

By substituting equation 25 into equation 24, the following equation can be made [22]:

$$\sigma^2 = \left(\frac{2D_T}{W}\right) X \quad (26)$$

This equation shows that σ^2 is proportional to time and to zone migration distance X. Giddings [22,27] states, that the coefficient $2D_T/W$ can be used as an index expressing the rate of growth of σ^2 along the separation path and giving it a symbol H to define separation power [22]

$$H = \frac{2D_T}{W} \quad (27)$$

By substituting into equation 26 the following equation can be expressed as:

$$H = \frac{\sigma^2}{X} \quad (28)$$

Which further can be expressed as [27,60]:

$$H = \frac{\sigma^2}{L} \quad (29)$$

Returning to the widely-established expression of number of theoretical plates equation:

$$H = \frac{L}{N} \quad (30)$$

Where H is now the plate height, L the length of the tubing or column, and N the number of theoretical plates, which can be also determined by the equation 6 in the previous part of this work relating to efficiency. This circle of dependency shows how the diffusion is related to the band broadening of the peak.

1.3.3 Dispersion

Dispersion is closely related to diffusion, therefore it can be mathematically described similar to that to diffusion [54]. The difference between diffusion and dispersion can be explained by external forces acting on the molecules in a macroscopic point of view. The dispersion effect is mostly independent from the chemistry, structure of the molecular weight of the molecules, but rather dependent on change in position caused by external forces such as flow [54].

In the situation of a laminar flow, the axial dispersion coefficient of the sample can be predicted. An often applied [61–65] equation on determining the dispersion coefficient is that from Taylor [66]. Taylor showed that the dispersion of one fluid into a circular capillary tube filled with a second fluid could be determined which he termed the dispersion coefficient K. This value

is not a physical constant but is dependent on the flow and its properties [61]. It is described as follows [66,67]:

$$K = \frac{a^2 U^2}{48D} \quad (31)$$

Where K is the dispersion constant, D is the molecular diffusivity, a is the radius of the pipe, U is the mean velocity and $1/48$ is a constant and a function of the profile of the flow. As it can be seen in the equation above, the diffusion coefficient from Fick is inversely proportional to the dispersion coefficient of Taylor. Furthermore, Taylor states that the above approximate solution (neglecting axial diffusion) is valid when the following condition is satisfied [61,67–69]:

$$\frac{4L}{a} \gg \frac{aU}{D} \gg 6.9 \quad (32)$$

Where L is the length of the pipe.

Aris modified Taylor's analysis to include axial diffusion and described the approximate solution as follows [61,68]:

$$K = D + \frac{a^2 U^2}{48D} \quad (33)$$

This equation is a better choice in the case when the axial and radial diffusion is significantly large (for very long capillaries or very low flow rates). This

equation can be re-written to better illustrate it in the form of variance that causes band broadening. By integrating the above equation and giving it a finite time of $t = 0$ to $t = L/U$ and L equals the total length of the capillary, it leads to [13]:

$$\sigma = \frac{2DL}{U} + \frac{a^2UL}{24D} \quad (34)$$

Where σ is the second central moment of the peak width at half height (see Figure 1).

Golay and Atwood have mentioned that the Taylor-Aris equation is only valid for pipes with a sufficient length and have shown in their experiments and analysis that the axial profile of the average concentration of the sample flowing in the tubing follows a complex evolution in shape due to the interaction of axial convection and radial diffusion [63]. Golay and Atwood [70] found that if the tubing is long there is ample time for radial diffusion to average each sample molecule's forward progress over the parabolic velocity distribution in the pipe. Thereby eluted peaks result in a Gaussian shape [70]. Furthermore, they stated that this equation does not apply for cases when the pipe is too short, the diffusivity of the sample is low, or the velocity is so high that there is not enough time for the velocity to average over the pipe resulting in a non-Gaussian peak shape [70,71]. They based their theory of band broadening, caused by diffusion, on the concept of the plate height theory [70]. The plate height theory can be applied to straight open

capillaries without the column. In order to determine the case where the sample plug in the flow does not have enough time to diffuse, for example, if the flowrate is much greater than the diffusion and dispersion time of the sample plug, the equation of Golay and Atwood can be applied to predict the optimal velocity of the flow. When the open capillary is treated as an open tubular column without retention, an optimum velocity F_{opt} , at which the height of a theoretical plate is at its minimum, can be expressed as follows [60]:

$$F_{opt} = \sqrt{48\pi D r_0} \quad (35)$$

Where D is the diffusivity of the sample in the mobile phase and r_0 is the radius of the tube. During the case where convection effect, due to Poiseuille flow, is greater than the axial dispersion of the sample, the following terms for dynamic diffusion apply [70]:

$$h = \frac{F}{24\pi D} \quad (36)$$

where h is the plate height and F the flow rate of the mobile phase. Using the above expression, the number of theoretical plates in a capillary of length L can be determined [70]:

$$n = \frac{L}{h} = \frac{24\pi D L}{F} \quad (37)$$

Where n is the number of theoretical plate, L is the length of the capillary. For long tubes where $n > 30$ the shape of the eluted peak is very close to Gaussian [70]. By using this number, it can be estimated if $F/F_{opt} \geq 30$ and therefore the number of theoretical plates will be so low that there is not time for diffusion because as the flow velocity increases the number of theoretical plate decreases.

2. Scope of the research

This dissertation is concerned about the separation science in high pressure liquid chromatography (HPLC). The focus in this research is to investigate and understand the fundamental aspect in the analytical separation science. It is known that extra column volume, mostly generated from the connecting tubing, the detector flow cell and the injector of the HPLC instrument, can cause band broadening, therefore affecting the overall separation quality, especially in the aspect of efficiency. It can be argued that the apparent increase of extra column volume would decrease the efficiency of the separation and cause an overall poor result.

This volume is needed to correct for the "real" retention volume V_R of the analyte which can be expressed with the following formula:

$$V'_R = V_R - (V_0 + V_{ex}) \quad (38)$$

Where V'_R = is the corrected retention volume of the analyte; V_R = the recorded retention volume of the analyte; V_0 = the column void volume and V_{ex} = the external column volume. The volume is considered as independent from the flow property, since the volume is a product of flow rate and retention time. Under this condition, the change of flow rate should not change the volume. Based on the law of conservation of matter, the volume entering the tubing should be the same as the volume exiting the tubing. During the research, a phenomenon has been encountered which was

expressed as an apparent increase of retention volume as a function of the increase of the mobile phase flow rate. The effect of an apparent increase in extra column volume, especially on the dependency of the flow rate in HPLC is of great concern. The goal of this research is to determine the cause of this apparent increase in extra column volume in multiple aspects of separation science. The first approach is to investigate the actual physical contribution from the connecting tubing to this effect. The different dimension of the connecting tubing, the mobile phase composition, and variations of the mobile phase flow rate will be also considered. Secondly, the research is following the idea of the contribution to this phenomenon through the diffusion behavior of the analyte. Third, it will continue to consider the possibility of the contribution to that phenomenon from the angle of the dispersion of the analyte sample caused by fluid motion through the tubing. Lastly, since the trend of HPLC instrumentation is going to be the miniaturization of the instrumentation as well as of the separation column, the findings will be discussed in the light of the new trend to try to improve the separation quality of the analysis. It is the hope that, at the very least, this research can provide insight into the separation science to recognize, understand, and isolate the unfavorable contribution of the extra column effect of the separation analysis, which will have much greater effect in smaller and shorter columns, minimally retentive analytes, and multi-systems setup such as LCxLC and LCxMS.

3. Experimental

3.1 Instrumentation and software

The retention volume analyses of the extra column volume were performed using a High Performance Liquid Chromatography from the Agilent/HP 1100 series HP-1100 (Agilent Technologies / Hewlett Packard Palo Alto, CA, USA) equipped with a degasser (Agilent/HP 1100 series G1322A), a binary pump (Agilent/HP 1100 series G1312A), an autosampler (Agilent/HP 1100 series G1313A), a column compartment (Agilent/HP 1100 series G1316A) and equipped with a variable wavelength UV-Vis detector VWD (Agilent/HP 1100 series G1314A). A refractive index detector (LC-30) from Perkin-Elmer (Norfolk, CT) was used instead of the VWD. The refractive index detector was connected to the HPLC through an interface from Agilent 35900E to enable communication between the detector and the HPLC instrumentation. Data acquisition was performed with ChemStation v. 10.0 software. Further analyses of the peaks were performed through Microsoft Excel. The raw data was exported from ChemStation as a CVS file and imported into Microsoft Excel.

For the experiments of the "super slow flow" and "stop flow", a Harvard Apparatus Model 22 syringe pump was used instead of the binary HPLC pump. A six-port Rheodyne valve was connected between the Harvard pump and the HPLC system. The injections of the samples were done through the HPLC

system. The syringe used in the Harvard 22 pump was a Hamilton glass syringe of the size of 5 ml.

3.2 Chemicals and material

Solvent used as mobile phases for the experiments were 100% HPLC grade acetonitrile (Pharmco, Brookfield, CT) and 100% HPLC grade methanol (Pharmco, Brookfield, CT). Purified water was supplied by an in-laboratory Milli-Q system (Millipore, Milwaukee, WI).

All PEEK tubing used for the experiments were from Upchurch Scientific (Oak Harbor, WA). Three different inner diameters of PEEK tubings (ID: 0.508 mm; 0.254 mm and 0.178 mm) were used with a consistent length of 914.4 mm (3 feet) throughout the entire experiment.

Samples used were deuterated acetonitrile (CD_3CN), methanol (CD_3OD), and water (D_2O) all from Sigma-Aldrich Co. (St. Louis, MO) each in the size of 1 ml vials.

3.3 Environment

All experiments were performed under ambient temperatures in the laboratory. PEEK tubing was connected and kept as straight as possible,

extra caution was taken to avoid applying stretching forces or sharp bends to the tubings, especially at the space directly after the fittings.

3.4 Experimental designs

3.4.1 Extra column volume measurements under normal condition

Accurate determination of the extra column measurements, in this case are crucial. In order to limit as much interference with the measurements as possible, it is important to choose an analyte / eluent combination with as little interaction as possible between the analyte and the eluent. With this consideration in mind, the deuterated form of the corresponding eluent was chosen to be the ideal candidate for the analyte. Since the focus was on the volume of the sample, the injection volume was chosen to be as small as possible without sacrificing the quality of the analysis. It was decided that an injection volume of 0.5 μl was an acceptable volume to ensure a reproducible and accurate injection of the HPLC system as well as a reliable and reproducible response from the refractive index detector. Injection volumes of the analyte were kept constant at 0.5 μl throughout the entire experiment. The tubing length of the PEEK tubing was kept constant at 914.4 mm (3 feet) and was connected directly from the injector outlet all the way to the detector inlet as one single piece of tubing as illustrated in Figure 6.

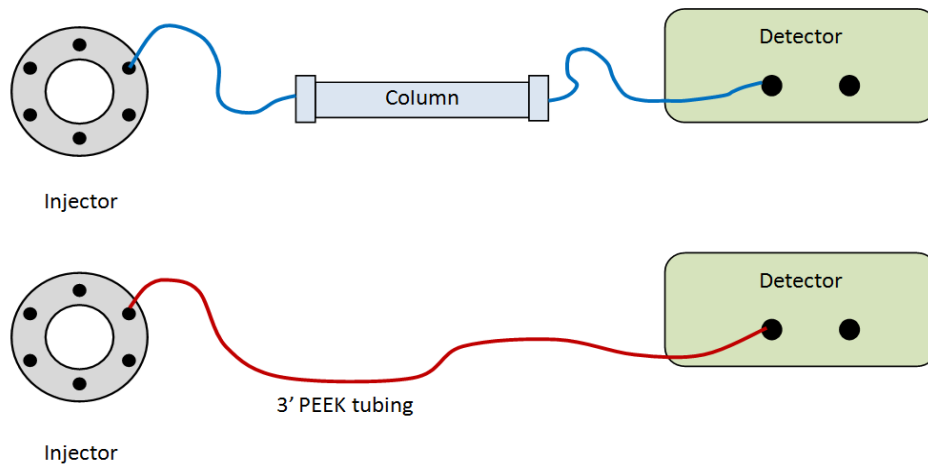


Figure 6: Illustration of the instrumental setup for the extra volume measurements. A single piece of tubing was used to connect the injector to the detector without a column.

After the injection of the deuterated sample, the peak maxima, as a function of time, were recorded. The value of the peak maxima was then assigned as the retention time t_R of the analyte. To express this peak maximum as the retention time t_R is of course a stretch of the true definition of retention time, but roughly speaking, if the time, in which the analyte travels within the tubing to be eluted after the injection were to be considered, it could be defined as retention time in the widest meaning.

The retention volume V_R is the product of the recorded retention time t_R of the injected analyte and the flow rate F . Injections were performed in triplicate and the flow rate F was varied (0.5 ml/min; 1 ml/min; 1.5 ml/min; 2 ml/min).

Three different mobile phases were chosen (methanol, acetonitrile, and water). The samples injected were the deuterated form of the mobile phase, e.g. 100 % methanol as mobile phase and the sample was 99.9 % deuterated methanol.

3.4.2 Extra column measurement under "super slow flow" conditions

For the "super slow flow" experiment, the Harvard Apparatus Model 22 syringe pump was used instead of the binary pump of the HPLC system. All tubings were PEEK tubings with an ID of 0.508 mm. Since this experiment focused on the flow rate, only one ID size of the tubing was utilized. The choice of the tubing ID of 0.508 mm was identified because this is the most

commonly used ID size in a regular HPLC system setup. The goal was to have an experimental setup in an environment as close as possible to a regular and common HPLC analysis setup. The flow rate was in the range from 0.01 ml/min to 0.001 ml/min. The syringe size of 5 ml was used, which contained the mobile phase. Base on the manufacturer's user manual, the nominal minimum and maximum flow rates of the 5 ml syringe is 0.0003 ml/min to 5.3 ml/min. The syringe operated well within its specifications. The pump accuracy and stability was checked by pumping purified water at 0.1 ml/min for 30 min and at 0.001 ml/min for 30 min into a 5 ml volumetric flask. The volumetric flow rate was determined by the mass of the water collected in the volumetric flask over time.

The samples were again the deuterated form of the mobile phase, e.g. 100% methanol as mobile phase and the sample was 99.9% deuterated methanol.

3.4.3 Extra column measurement under "stop flow" conditions

For the "stop flow" experiment, the Harvard Apparatus Model 22 syringe pump was again used instead of the binary pump of the HPLC system. The sample was injected into an extra loop connected on the six-port valve as shown in Figure 7. The connecting tubing including the loop were made from PEEK with an ID of 0.508 mm. This size ID was chosen to be consistent with the previous super slow flow experimentation. The loop was 914.4 mm long. The syringe size, which contained the mobile phase, was 5 ml.

Positions on the six-port Rheodyne valve (see also Figure 7):

ON position:

Mobile phase (green line), coming from the pump, enters at position (3), travels to position (2) through the loop at positions (2 to 5) (red line) and out at position (4) into the detector

Injector/sample line (orange) comes from the syringe and enters at position (1) through position (6) and then out to waste bypassing the loop (red line).

OFF position:

Mobile phase (green line) comes from the pump and enters at position (3) flows directly to the detector at position (4) bypassing the loop

Injector/sample line (orange) comes from the syringe and enters at position (1) over position (2) where it fills the loop at position (2 to 5) and from (5) to (6) directly to waste.

During the stop flow condition, the injected sample experienced a dwell time within the loop. During the dwell time of the analyte, the six-port valve was at the OFF position.

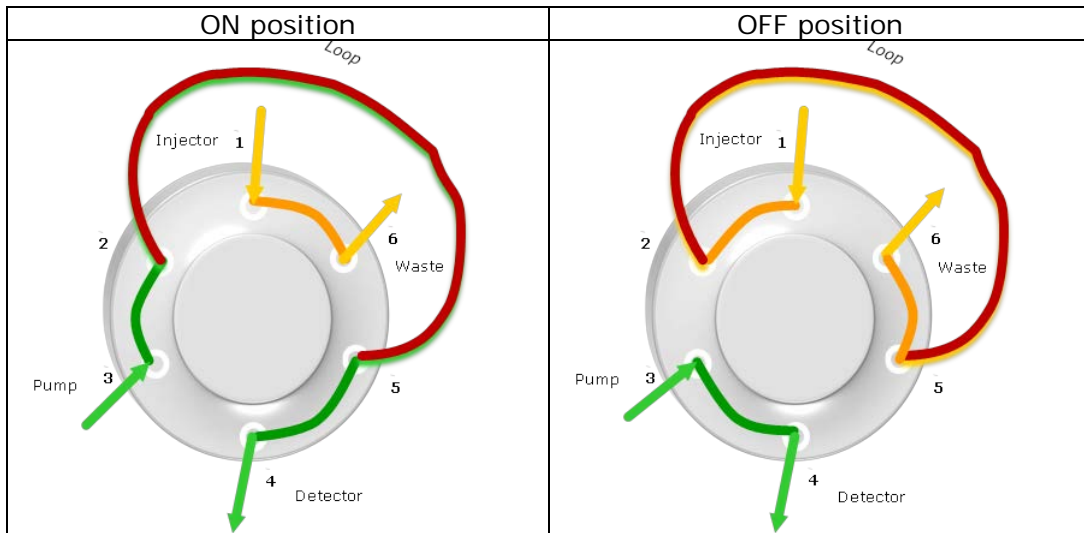


Figure 7: Illustration of the 6-port valve. On the left the switch is on the ON position and on the right side, the switch is on the OFF position.

4. Results and Discussion

The goal of the research was to investigate the apparent increase of retention volume in dependency of the flow rate during the external column volume determination. As stated previously, the external column volume should stay constant regardless of the flow rate. The experiments on the other hand show a dependency of the apparent increase of the retention volume with the flow rate. Multiple different measurements have been performed to evaluate this case and to find an explanation. The results of those experiments are listed in the order of performance.

- I. Comparison between three different mobile phases and different flow rates to explore if there is a correlation between mobile phase and/or flow rate
- II. Comparison between tubing with different inner diameters
- III. Comparison between PEEK tubing and stainless steel tubing to explore the possibility of dependency of tubing material
- IV. Comparison of flow rate at a greater range between very high and very low flow rates
- V. Investigation of contribution to this effect through diffusion
- VI. Investigation of contribution to this effect by diffusion through the fluid flow profile through the tubing

4.1 Zone marker migration comparison between mobile phases and variation of the flow rate

Three different mobile phases (acetonitrile, water, and methanol) were compared with each other and with the flow rates varied from 0.5 ml/min to 2.0 ml/min in 0.25 ml/min increments. The samples used were the deuterated form of the respective mobile phases. The results in Table 1, Table 2, and Table 3 demonstrate the trend of increasing retention volume by increasing flow rate. These results are shown for the PEEK tubing with ID of 0.178 mm (0.007 inches) and a length of 914.4 mm (3 feet). The apparent increase of volume lies in the vicinity of 40 μ l, when examined from the lowest flow rate to the highest flow rate. This apparent increase of volume was consistent throughout the three different mobile phases.

After plotting the data together as illustrated in Figure 8 it can be seen that there is practically a linear increase of the apparent retention volume with no significant difference in the retention volume VR variation between the three different mobile phases.

Table 1: Retention volume of deuterated acetonitrile in 100 % acetonitrile mobile phase at various flow rates. An increase of the retention volume of 31 μl has been recorded when the retention volume was measured from the lowest flowrate to the highest flowrate and then compared.

Mobile phase: Acetonitrile						
Line condition: length = 914.4 mm; ID = 0.178 mm						
Sample: deuterated acetonitrile CD ₃ CN						
Flowrate F [ml/min]	Retention Time t_R [min]			Avg t_R [min]	Retention Volume V_R [ml]	Pressure P [bar]
0.50	0.182	0.183	0.183	0.183	0.091	4
0.75	0.129	0.130	0.129	0.129	0.097	5
1.00	0.102	0.102	0.102	0.102	0.102	6
1.25	0.086	0.086	0.086	0.086	0.108	8
1.50	0.075	0.075	0.075	0.075	0.113	10
1.75	0.067	0.067	0.067	0.067	0.117	11
2.00	0.061	0.061	0.061	0.061	0.122	12
Volume difference $V_{R, \text{highest}} - V_{R, \text{lowest}}$					0.031	

Table 2: Retention volume of deuterated water in 100% water mobile phase at various flow rates. An increase of the retention volume of 39 μl has been recorded when the retention volume was measured from the lowest flowrate to the highest flowrate and then compared.

Mobile phase: Water						
Line condition: length = 914.4 mm; ID = 0.178 mm						
Sample: deuterated water D ₂ O						
Flowrate F [ml/min]	Retention Time t_R [min]			Avg t_R [min]	Retention Volume V_R [ml]	Pressure P [bar]
0.50	0.183	0.183	0.183	0.183	0.092	9
0.75	0.131	0.130	0.131	0.131	0.098	13
1.00	0.104	0.104	0.104	0.104	0.104	17
1.25	0.088	0.088	0.088	0.088	0.110	20
1.50	0.077	0.077	0.076	0.077	0.116	24
1.75	0.069	0.069	0.069	0.069	0.121	28
2.00	0.067	0.065	0.064	0.065	0.131	32
Volume difference $V_{R, \text{highest}} - V_{R, \text{lowest}}$					0.039	

Table 3: Retention volume of deuterated methanol in 100% methanol mobile phase at various flow rates. An increase of the retention volume of 40 μl has been recorded when the retention volume was measured from the lowest flowrate to the highest flowrate and then compared.

Mobile phase: Methanol						
Line condition: length = 914.4 mm; ID = 0.178 mm						
Sample: deuterated methanol CD ₃ OD						
Flowrate F [ml/min]	Retention Time t_R [min]			Avg t_R [min]	Retention Volume V_R [ml]	Pressure P [bar]
0.50	0.182	0.182	0.181	0.182	0.091	10
0.75	0.136	0.134	0.136	0.135	0.102	14
1.00	0.107	0.107	0.107	0.107	0.107	19
1.25	0.091	0.091	0.091	0.091	0.114	24
1.50	0.079	0.080	0.079	0.079	0.119	29
1.75	0.071	0.072	0.072	0.072	0.125	33
2.00	0.066	0.065	0.065	0.065	0.131	38
Volume difference $V_{R, \text{highest}} - V_{R, \text{lowest}}$					0.040	

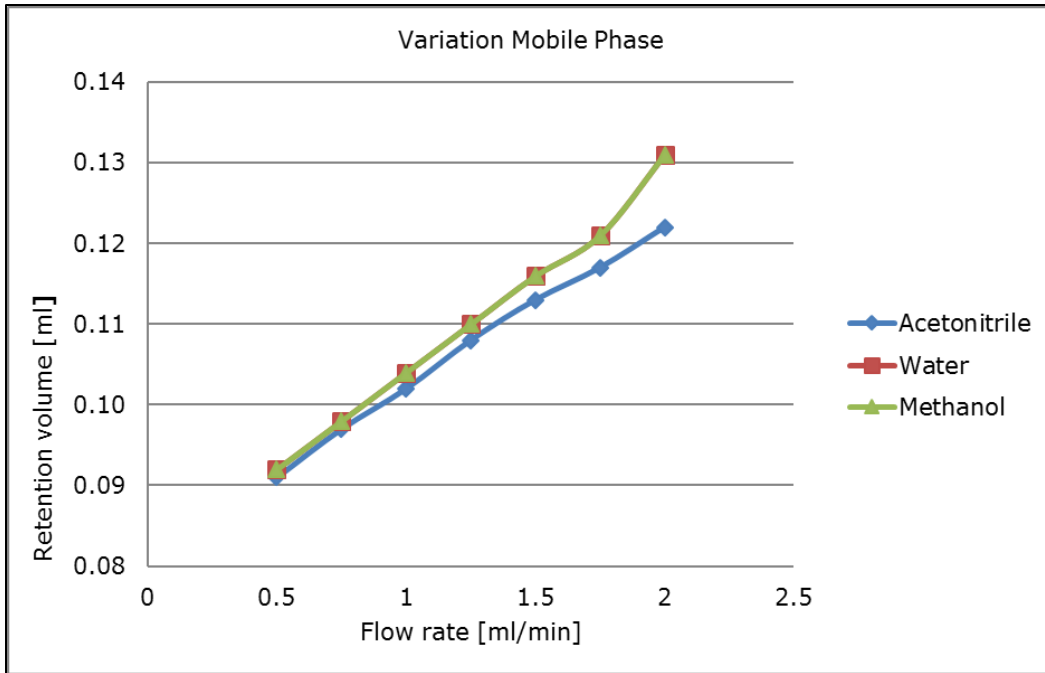


Figure 8: Comparison of different mobile phases at different flow rates with tubing length of 914.4 mm and ID 0.178 mm. The differences in retention volume between the three different mobile phases are very small when compared to the change of volume caused by the flow rate.

The difference in retention volume V_R of the analyte between acetonitrile, water, and methanol is insignificant when compared to the retention volume change apparently caused by the flow rate. For example, at the flow rate of 1 ml/min, the resulting V_R of the analytes are 0.102 ml, 0.104 ml and 0.107 ml (acetonitrile, water, and methanol respectively) and do not show a great difference, however, evidently the trend of apparent increase of V_R persist throughout the experiment. In the case of methanol, the retention volume apparently increased from 0.091 ml to 0.131 ml, which is an increase in volume of 40 μ l, which means an increase of about 132 %. In order to investigate the effect of the apparent increase of V_R , a different approach was taken to have a closer look into this phenomenon.

4.2 Variation of inner diameter of PEEK tubing

Retention volume changes in dependency of the flow rate were investigated on three different PEEK tubing with consistent lengths of 914.4 mm (3 feet) but different inner diameters (ID 0.508 mm, 0.254 mm and 0.178 mm). The effect of the apparent increase of retention volume is shown on all three different inner diameter tubing as it can be seen in Figure 9. The difference in retention volume changes seen between the three tubing ID's is not very significant. All three data series, of the different mobile phases, have a very similar slope and exhibit a very linear relationship to the flowrate. Since the data represent the retention volumes, which were calculated from the

respective retention times, it does not reflect the actual tubing volume. By decreasing the tubing inner diameter by half from 0.508 mm to 0.254 mm for example, the theoretical volume of the tubing with the same length will decrease to one fourth of the volume. To be able to compare the different tubing, the data need to be normalized against the actual tubing volume for a better representation. The theoretical volume of the tubing is calculated by:

$$V_{cylinder} = \pi * r^2 * L \quad (39)$$

where $V_{cylinder}$ = volume of tubing; r = radius of tubing; L = length of tubing

Table 4 shows the results of retention volumes measured at different flow rates F [ml/min], different inner diameter [ID] and different mobile phases. The listed retention volume reflects the average of retention time from triplicate measurements.

Table 4: Variation of tubing ID with the retention volume measured at different flow rates of different mobile phases. Data displayed is the average retention volume of triplicate measurements.

Average retention volume of mobile phases [ml]									
	ID 0.508 mm			ID 0.254 mm			ID 0.1778 mm		
F [ml/min]	ACN	MeOH	H ₂ O	ACN	MeOH	H ₂ O	ACN	MeOH	H ₂ O
0.50	0.265	0.254	0.256	0.118	0.118	0.118	0.091	0.091	0.092
0.75	0.272	0.257	0.261	0.124	0.125	0.125	0.097	0.102	0.098
1.00	0.279	0.256	0.268	0.130	0.132	0.132	0.102	0.107	0.104
1.25	0.284	0.257	0.258	0.135	0.138	0.138	0.108	0.114	0.110
1.50	0.291	0.267	0.267	0.141	0.144	0.145	0.113	0.119	0.116
1.75	0.296	0.275	0.277	0.147	0.152	0.153	0.117	0.125	0.121
2.00	0.301	0.282	0.286	0.155	0.158	0.159	0.122	0.131	0.131
Volume difference $V_{R, \text{highest}} - V_{R, \text{lowest}}$									
	0.036	0.028	0.030	0.037	0.040	0.041	0.031	0.040	0.039

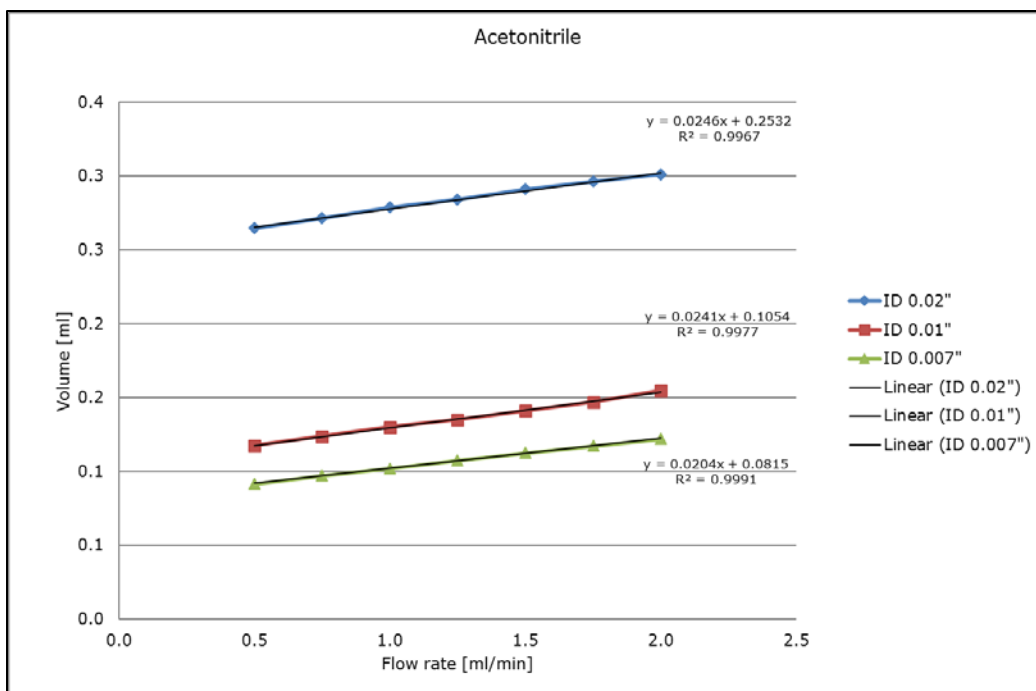


Figure 9: Retention volume of deuterated acetonitrile in acetonitrile mobile phase. Comparison of V_R between different inner diameters of the tubing (0.02" = 0.508 mm, 0.01" = 0.254 mm, 0.007" = 0.178 mm).

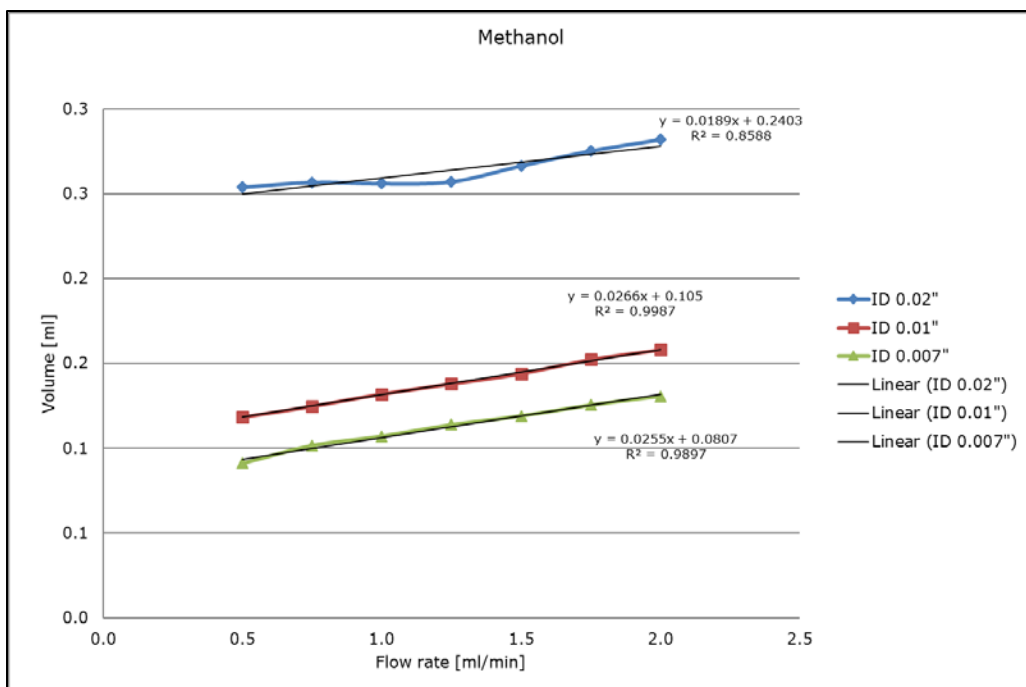


Figure 10: Retention volume of deuterated methanol in methanol mobile phase. Comparison of V_R between different inner diameters of the tubing (0.02" = 0.508 mm, 0.01" = 0.254 mm, 0.007" = 0.178 mm).

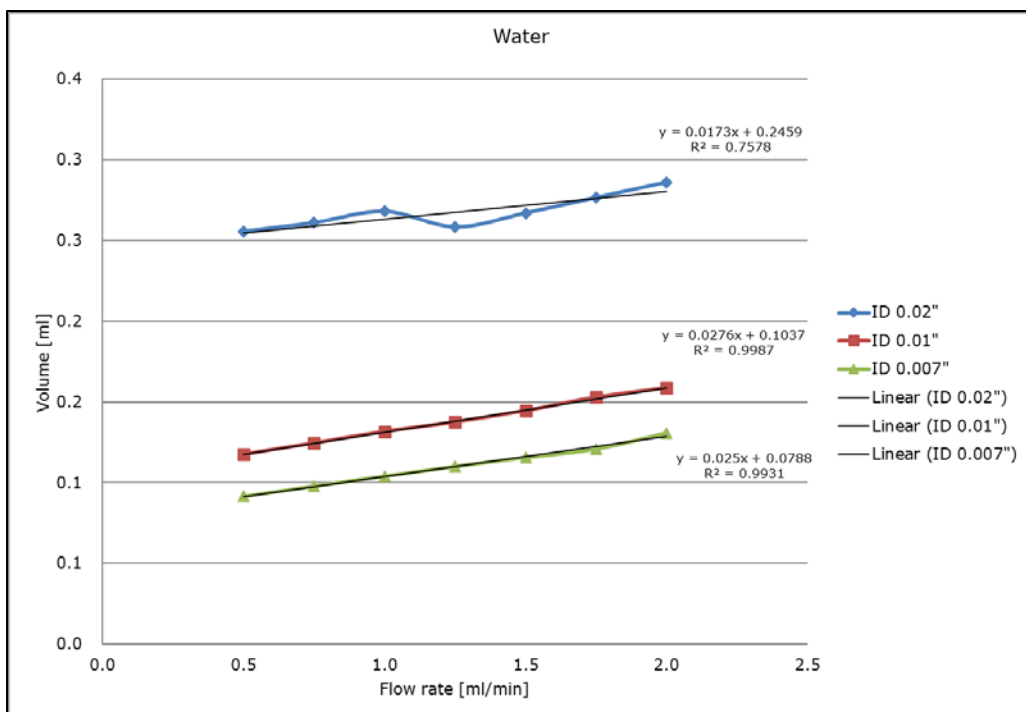


Figure 11: Retention volume of deuterated water in water mobile phase.

Comparison of V_R between different inner diameters of the tubing

(0.02" = 0.508 mm, 0.01" = 0.254 mm, 0.007" = 0.178 mm).

Table 5 is the normalized data of the retention volume against the actual volume of the tubing. The results were obtained by the following calculation:

$$N = (V_{avg} - d)/V_{cylinder} \quad (40)$$

were N = normalized value; V_{avg} = average of all V_R ; d = difference

The average V_{avg} was obtained by taking the average of all $V_{R[ID]}$ within the column representing the ID of interest. The difference is the value obtained by subtracting the V_{avg} with $V_{cylinder}$.

The normalization of the data made it possible to compare the three different tubing with each other. In the case of acetonitrile for example, the slope of the data series in comparison between the different tubing ID (see Figure 9) was originally very similar, around 0.02x where the biggest ID exhibited the steepest slope of 0.0246x, which could lead to the assumption that the different tubing ID would not cause a noticeable apparent volume increase of the retention volume. After normalizing the data against the nominal value of the tubing, the tubing with the smallest ID now exhibits the steepest slope with a value of 0.8998x (see Figure 12), which leads to a finding that a tubing with a smaller ID in comparison to a tubing with a greater ID seems to have a greater effect on the apparent increase of retention volume, additionally to the change of flow rate.

Table 5: Normalized data of the measured retention volume against the actual tubing volume.

Normalized data									
	ID 0.508 mm			ID 0.254 mm			ID 0.178 mm"		
F [ml/min]	ACN	MeOH	H2O	ACN	MeOH	H2O	ACN	MeOH	H2O
0.50	0.962	0.903	0.913	0.573	0.591	0.573	0.182	0.167	0.189
0.75	0.998	0.919	0.942	0.708	0.729	0.724	0.431	0.629	0.470
1.00	1.037	0.915	0.980	0.842	0.886	0.878	0.651	0.872	0.739
1.25	1.067	0.921	0.927	0.950	1.013	1.004	0.894	1.169	1.004
1.50	1.104	0.971	0.974	1.080	1.145	1.155	1.114	1.400	1.246
1.75	1.132	1.019	1.025	1.209	1.323	1.335	1.323	1.683	1.477
2.00	1.159	1.055	1.077	1.375	1.447	1.461	1.532	1.914	1.914
Volume difference $V_{R, \text{highest}} - V_{R, \text{lowest}}$									
	0.197	0.152	0.164	0.802	0.856	0.888	1.350	1.747	1.725

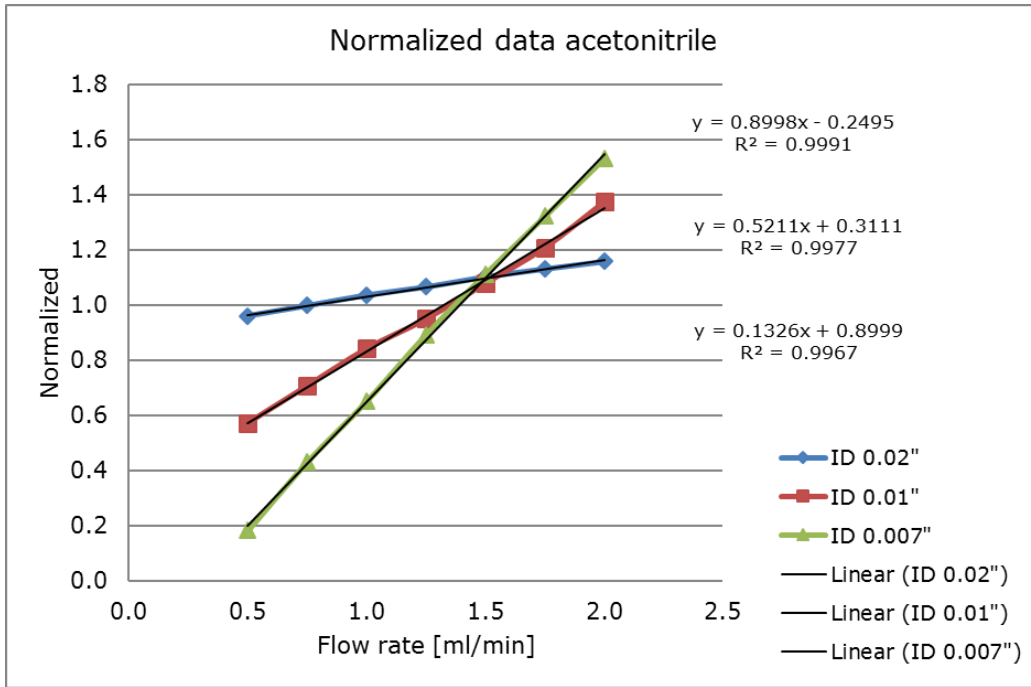


Figure 12: Normalized data of measured retention volume and theoretical tubing volume (0.02" = 0.508 mm, 0.01" = 0.254 mm, 0.007" = 0.178 mm).

Overviewing all data so far, an approximation of the retention volume for tubing with ID of 0.127 mm can be made by using the following formula from the graph (Figure 9, Figure 10 and Figure 11).

$$y = ax + b \quad (41)$$

$$y_{ID\ 0.005} = 0.023x + 0.060 \quad (42)$$

Table 6: Approximation for the retention volume on tubing with ID of 0.127 mm. The values are the averages of the three different mobile phases from the previous experiment variation of tubing ID using the equation displayed on the graphs.

Approximation for retention volume on tubing with ID of 0.127 mm				
ID	ID reduced by	a	b	b reduced by
0.020		0.020	0.246	
	-50%			-57%
0.010		0.026	0.105	
	-30%			-25%
0.007		0.024	0.080	
	-30%			-25%
0.005		0.023	0.060	

Table 7: Increase of the apparent retention volume as percentage in dependency of the flow rate. The trend is more pronounced in tubing with smaller ID.

Percental increase of apparent retention volume in dependency of the flow rate								
	Tubing ID							
	0.508 mm		0.254 mm		0.178 mm		0.127*	
F	V _R	%	V _R	%	V _R	%	V _R	%
0.5	0.265		0.118		0.091		0.072	
		+5		+10		+12		+15
1.0	0.279		0.130		0.102		0.083	
		+8		+19		+20		+28
2.0	0.301		0.155		0.122		0.106	

* values are approximated, not actual measurement.

4.3 Stainless Steel Tubing

Stainless steel tubing is often used in HPLC instead of PEEK tubing. The purpose of this experiment was to investigate whether the effect of increasing retention volume noticed on the previous experiment with PEEK tubing would appear in the case of stainless steel tubing as well.

Measurement on conventional stainless steel tubing for HPLC applications was done with two different mobile phases, acetonitrile, and water. Based on the measurements done and after evaluation of the recorded data (see Table 8 and Table 9), it seems the effect of increasing volume is also noticeable on stainless steel tubing.

Stainless steel unfortunately was a little unsuited for further experiments, since it would provide some difficulties in changing the tubing length. PEEK tubing on the other hand provides a more manageable material in the perspective on cutting the tubing in the length required for experimentation. Since the stainless steel tubing demonstrated similar trend as in the case of PEEK tubing and even different mobile phase demonstrated the same trend, further experiments on stainless steel was discontinued.

Table 8 and Table 9 summarize the data of retention volume measurements at different flow rate conditions with acetonitrile and water on stainless steel HPLC connecting tubing. The comparison of retention volume of deuterated samples between acetonitrile and water is graphed in Figure 13.

Table 8: Summarizes the data of retention volume measurements at different flow rate conditions with acetonitrile on stainless steel HPLC connecting tubing.

Mobile Phase: Acetonitrile					
Stainless Steel Tubing ID = ~0.381 mm; length 2 m					
Sample: Deuterated acetonitrile					
F [ml/min]	Retention time [min]			Ave t_R [min]	V_R [ml]
0.10	3.127	3.125	3.125	3.126	0.313
0.25	1.252	1.252	1.251	1.252	0.313
0.50	0.634	0.635	0.635	0.635	0.317
0.75	0.429	0.430	0.429	0.429	0.322
1.00	0.327	0.327	0.327	0.327	0.327
1.25	0.266	0.265	0.265	0.265	0.332
1.50	0.224	0.225	0.225	0.225	0.337
1.75	0.195	0.195	0.195	0.195	0.341
2.00	0.173	0.173	0.173	0.173	0.346

Table 9: Summarizes the data of retention volume measurements at different flow rate conditions with water on stainless steel HPLC connecting tubing.

Mobile Phase: Water					
Stainless Steel Tubing ID = 0.381 mm; length 2 m					
Sample: Deuterated Water					
F	Retention Time			Ave t_R	V_R
0.10	2.932	2.930	2.934	2.932	0.293
0.25	1.179	1.179	1.184	1.181	0.295
0.50	0.596	0.597	0.593	0.595	0.298
0.75	0.403	0.402	0.399	0.401	0.301
1.00	0.304	0.305	0.305	0.305	0.305
1.25	0.249	0.248	0.249	0.249	0.311
1.50	0.211	0.212	0.210	0.211	0.317
1.75	0.184	0.185	0.185	0.185	0.323
2.00	0.164	0.164	0.165	0.164	0.329

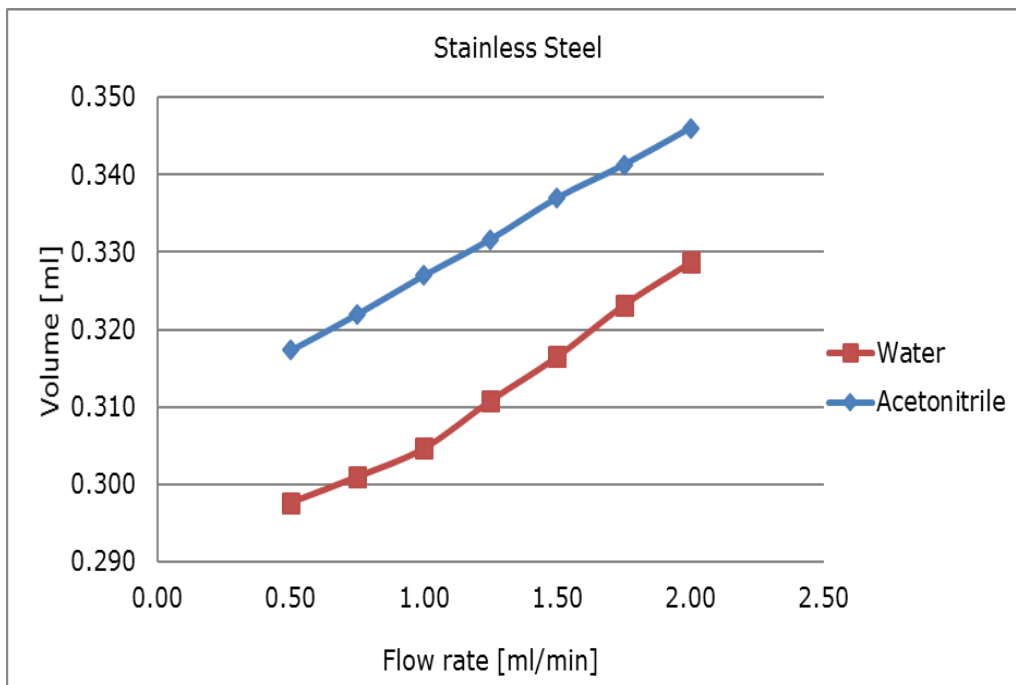


Figure 13: Retention volume versus flow rate on stainless steel tubing with acetonitrile and water.

4.4 Greater Range

The trend observed so far was that the retention volume would apparently increase by increasing the flow rate and this effect was independent of the mobile phase or the tubing property in respect of the tubing material PEEK versus stainless steel. The new question was if there would be an upper and lower limit of the flow rate where the apparent increase of retention volume would not become a noticeable effect. The hypothesis so far is that, first, at some point of the higher flow rate range, the apparent increase of volume should reach its plateau, since it is evidently not possible to have an indefinitely large volume. The second presumption is that by slower flow rate, the injected sample volume or sample plug will have more resident time within the tubing and will therefore spread by the means of diffusion. Since the sample volume within the tubing will be surrounded with the mobile phase, it is naturally to expect a concentration gradient between the sample (deuterated) and the mobile phase causing diffusion of the sample, which will cause a greater overall sample plug volume. The thought was that the greater the resident time of the sample in the tubing, the more time the sample will have to diffuse and therefore, the diffusion will cause such a zone spreading which will be registered as band broadening of the retention peak in chromatographic environment, presenting a resulting in an apparent greater retention volume.

The new flow rate range now is from 0.01 ml/min up to 2 ml/min. Comparison of measured retention volume within this broader range is illustrated in Figure 14 and Figure 15. The tubing used in this experiment was PEEK tubing with an ID of 0.254 mm and 0.508 mm. The mobile phase was acetonitrile and the sample was deuterated acetonitrile.

To be able to overlay the peaks obtained through different flow rates, the data are represented in retention volume to response. The retention volume V_R was obtained by the following calculation:

$$V_R = t_R * F \quad (43)$$

Where V_R is the retention volume, t_R is the retention time of the analyte and F is the volumetric flow rate.

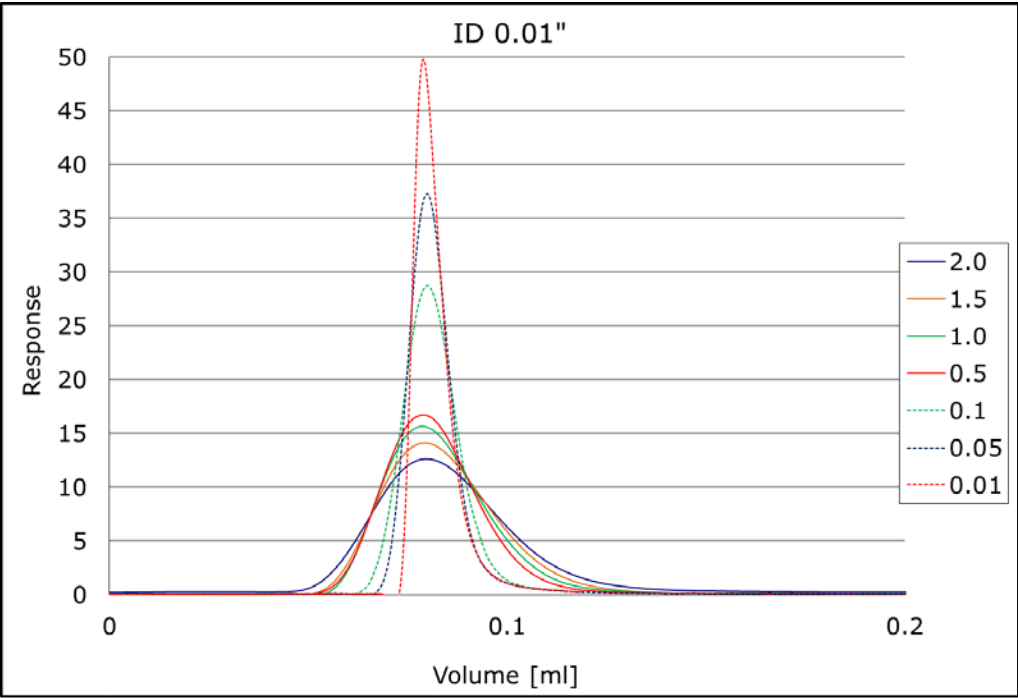


Figure 14: Elution profile comparison of different flow rate from 0.01 ml/min up to 2 ml/min graphed as volume to response on tubing with ID of 0.254 mm.

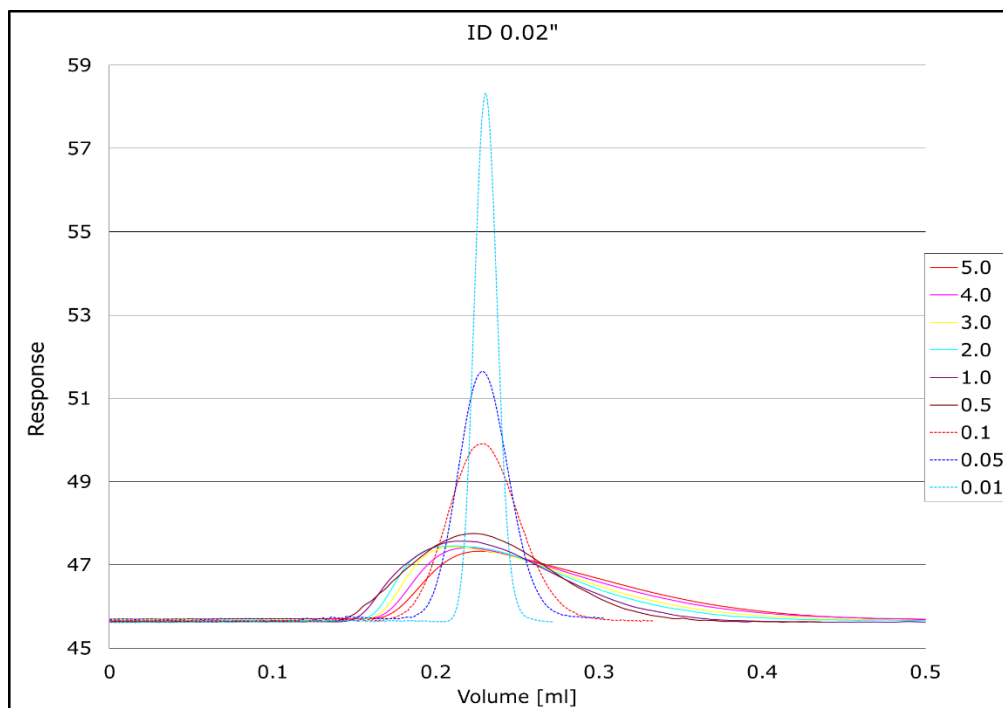


Figure 15: Elution profile comparison of different flow rate from 0.01 ml/min up to 5 ml/min graphed as volume to response on tubing with ID of 0.508 mm.

On the first view, it seems that those experiments are following the same trend as noticed in the previous experiment (4.2 *Variation of inner diameter of PEEK tubing*). The effect appears to be more prevalent with tubing of smaller ID than tubing with bigger ID. Nevertheless, the data acquired was unexpected. As mentioned earlier, the hypothesis was that at slower flow rate the peak would broaden through the contribution of the diffusion effect. Consequently, the peak shape of the flow rate at the higher region would be narrower. It can be seen in Figure 14 and Figure 15 that it is not the case as expected. The plateau for the apparent increase of retention volume appears to be reached at already 0.5 ml/min flow rate. Based on the graph there is no visible differences in retention volume between 0.5 ml/min and 5.0 ml/min. However, we know from the previous experiment that between 0.5 ml/min and 5.0 ml/min flow rate, there is a noticeable apparent increase in retention volume. It is not very visible base on the scale of the figure. The same results are illustrated again in Figure 16 and Figure 17. In this case, the fast flow and slow flow region were illustrated separately to have a clearer view of the peaks.

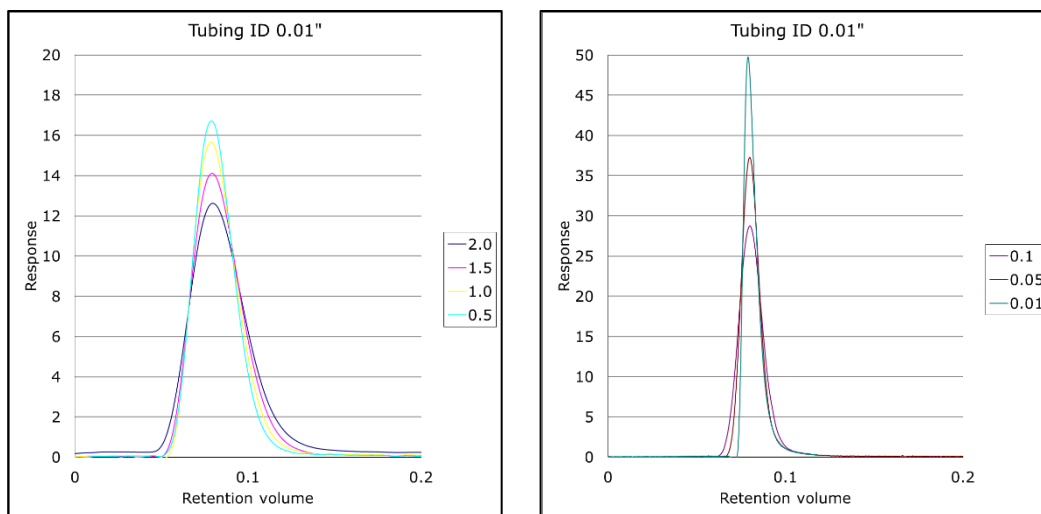


Figure 16: Elution profile graphed in retention volume against response comparison of different flow rates. On the left from 0.5 ml/min to 2 ml/min and on the right side from 0.01 ml/min to 0.1 ml/min. Both on tubing with ID of 0.254 mm.

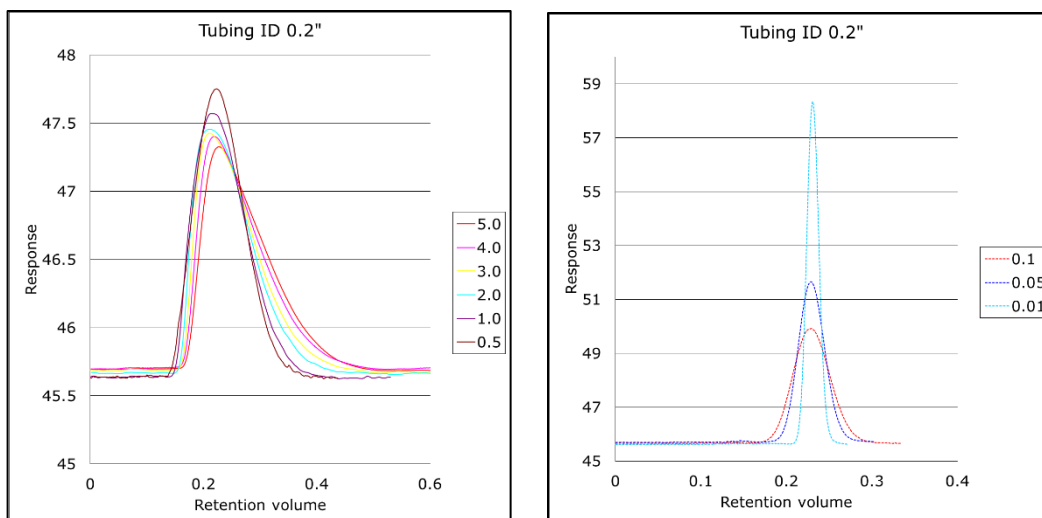


Figure 17: Elution profile graphed in retention volume against response comparison of different flow rates. On the left from 0.5 ml/min to 5 ml/min and on the right side from 0.01 ml/min to 0.1 ml/min. Both on tubing with ID of 0.508 mm

It can be seen in the previous experiment, that the peak shape at higher flow rate are not as symmetrical as the peaks in the lower flow rate region. In Figure 18 the summary of peaks, the peaks were plotted individually by time. To have a better representation of the experimental data, only the corrected peak width was plotted against the flow rate (see Figure 19). The peak width was corrected for the flow rate for easier comparison (see Table 10) by determining the measured peak width in minutes and multiplying that value with the corresponding flow rate.

The interesting component of Figure 19 is that it demonstrates the increase of peak width in dependency of the increase of flow rate in a close manner to the logarithmic trend line which leads to the assumption that the rate of change in peak width (increasing peak width) is higher within the lower region of the flow rate and that it almost levels out at the higher region of the flow rate. The comparison in the perspective of volume however shows a linear relationship to the increase of flow rate suggesting a steady rate of change. The assumption that the apparent increase of retention volume will level out eventually is supported by the data shown in Figure 19 but it still does not explain the change of retention volume or the peak width in dependency on the flow rate.

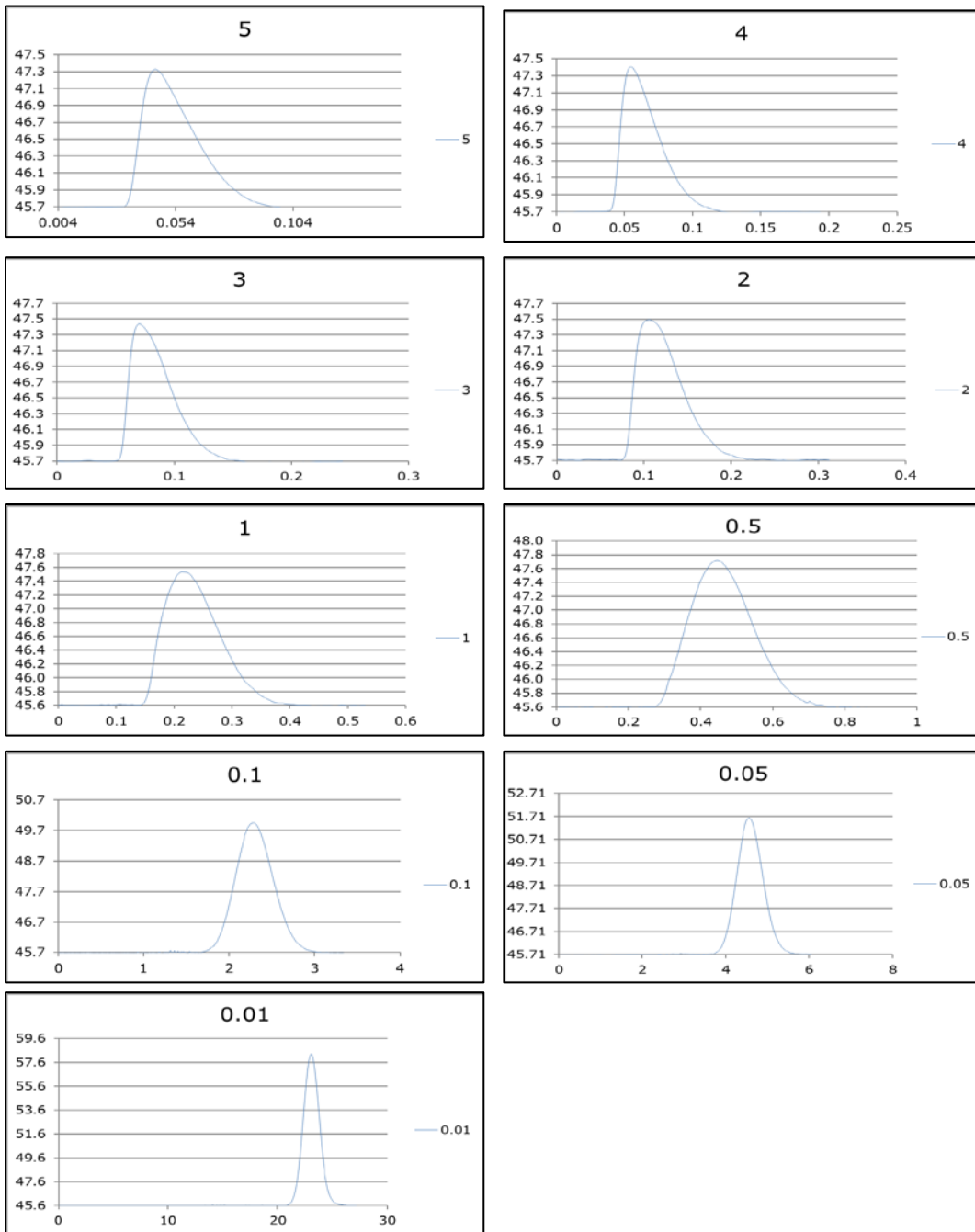


Figure 18: Summarization of individual peaks at different flow rate (shown on chart title). Y axis is the response and the x axis the retention time in min.

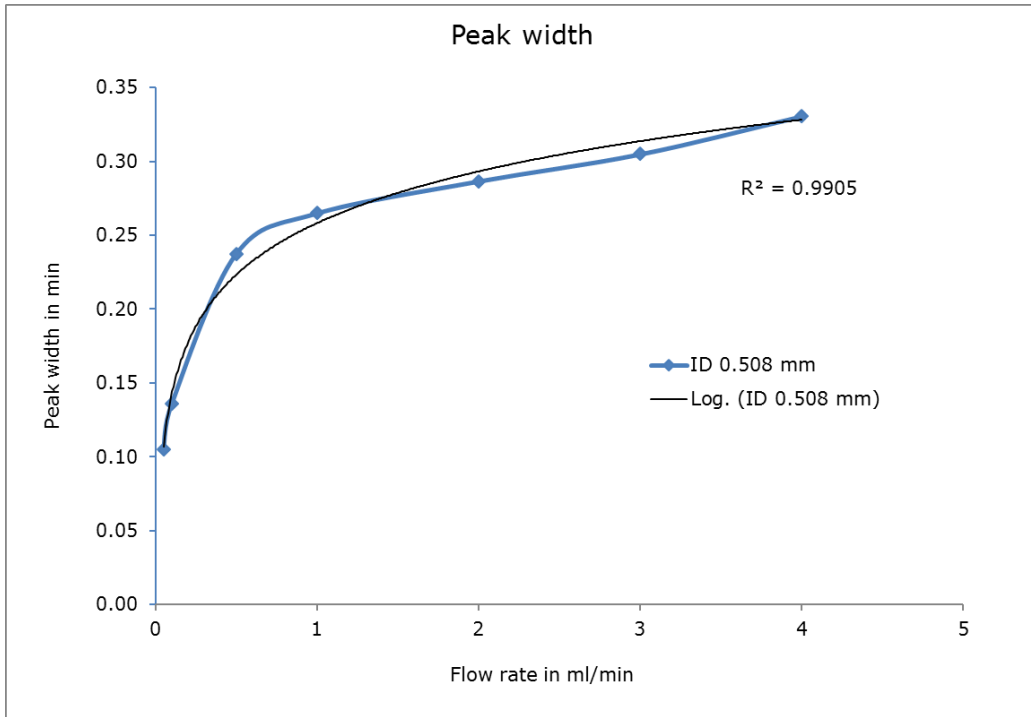


Figure 19: The graph illustrates the change of the peak width in relation to the change of the flow rate. The peak width is corrected for the flow rate. This is a clearer demonstration that the peak width increases with the increase of velocity.

Table 10: Measured and calculated value for peak width dependency on flow rate.

Greater range experiment				
F [ml/min]	Peak start at time t [min]	Peak end at time t [min]	Peak width [min]	Product of Peak width and F
4.00	0.0366	0.1192	0.0827	0.331
3.00	0.0476	0.1492	0.1017	0.305
2.00	0.0712	0.2145	0.1433	0.287
1.00	0.1368	0.4018	0.2650	0.265
0.50	0.2648	0.7398	0.4750	0.238
0.10	1.6423	2.9990	1.3567	0.136
0.05	3.6357	5.7357	2.1000	0.105

4.5 Super Slow Flow

The super slow flow was done with a Harvard 22 apparatus syringe pump instead of the pump from the HPLC system. This pump could provide a steady flow at a very low velocity. Three different flow rates were chosen (0.005 ml/min, 0.0025 ml/min, and 0.001 ml/min). The results show no significant difference in peak width when corrected for flow rate. Based on the previous experiment and the new results, it can be seen that the peak broadening is nonlinear. Since the peak width did not appear to change significantly, a new experiment was started. The results of this experiment are illustrated in Figure 20 and summarized in Table 11.

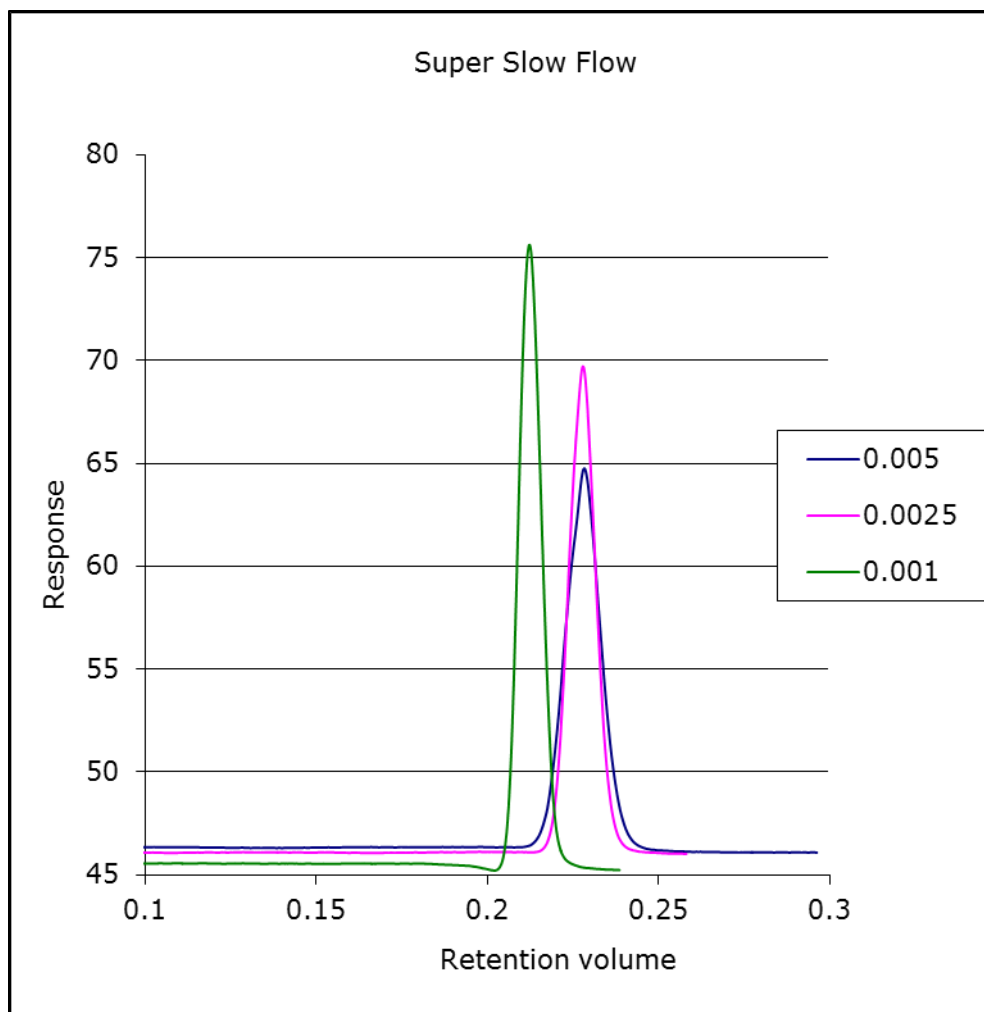


Figure 20: Measurement of retention volume in dependency of flow rate from 0.001 ml/min to 0.005 ml/min normalized for volume.

Table 11: Measured and calculated value for peak width dependency on velocity.

Super slow flow experiment				
F [ml/min]	Peak start at time t [min]	Peak end at time t [min]	Peak width [min]	Product of Peak width and F
0.005	42.075	49.658	7.583	0.038
0.0025	85.567	98.983	13.416	0.034
0.001	201.792	235.792	34.000	0.034

4.6 Stop Flow

The next experiment was a so-called “stop flow” experiment. The purpose of this experiment was to have the analyte “dwell” in an undisturbed environment to give it time to diffuse. The sample was injected and the six-port valve was on the –OFF- position allowing the sample to reach the loop (PEEK tubing with ID of 0.508 mm and 914.4 mm length), which was bigger (tubing volume is 25.4 μ l) than the sample volume of 0.5 μ l. After the first injection, the retention time of the analyte traveling through the loop was recorded (see Figure 7 for illustration). The time was estimated, based on the retention time, where the sample plug would be residing in the middle of the loop (traveling half the distance of the loop). After the first determination, sample was then “parked” in the loop and the valve was switched to –ON-, so the mobile phase would bypass the sample loop. After a predetermined time of “sample dwell time” the valve was then switched again to the -OFF-, where the mobile phase would pass through and elute the sample in the loop. The flow rate to “fill” the loop and the flow rate of eluting the loop were kept the same throughout the experiment at 0.01 ml/min. This setup was chosen to limit any pressure and velocity fluctuation, by eliminating the necessity to turn the pump off and on again. Therefore, by using the six-port valve, the flow was undisturbed and was deviated to the other line when the sample was ready to be eluted.

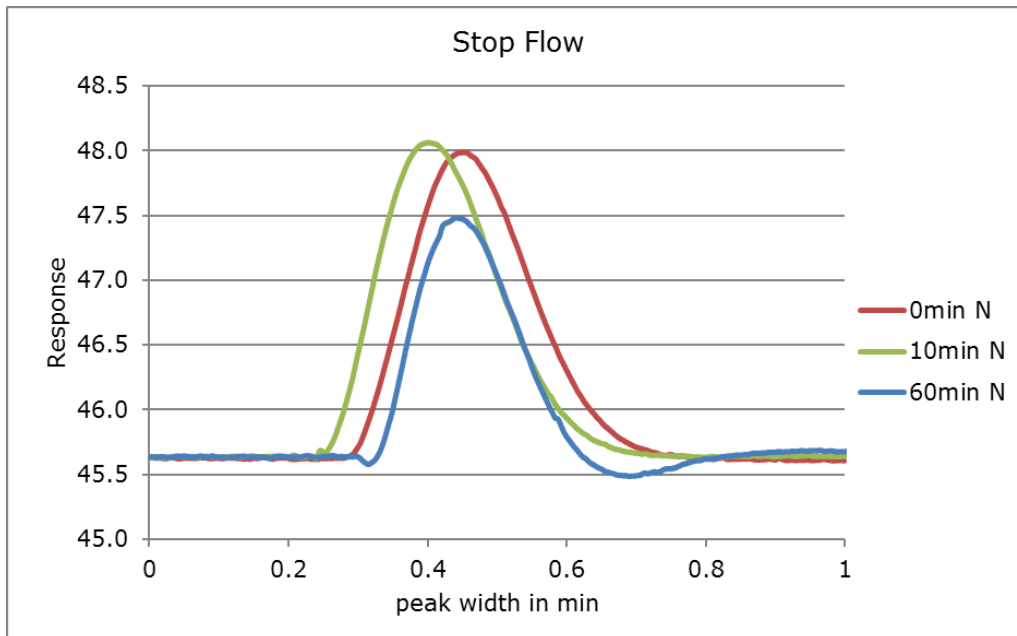


Figure 21: Peak broadening experiment under stop flow conditions showing peaks from three different dwell times in loop. The peaks were corrected for the time delay.

The position of the peaks were corrected for the time delay, meaning that the time prior to the elution of the sample from the peak was cut out for better visualization. For peak 10 min N the first 10 min recorded were cut out as well for the peak 60 min N, the first 60 min were disregarded. It was surprising to see that the difference in the peak widths was very low. The hypothesis was that the peak width of the sample would increase with increasing dwell time in the tubing due to longitudinal diffusion, giving the sample plug enough time to diffuse. The results shown in Figure 21 suggest that longitudinal molecular diffusion is practically insignificant in regards of the band broadening.

Main conclusion from these experiments is that the combination of radial diffusion within the laminar flow profile is the major factor in band broadening as shown in Figure 14 to Figure 17.

4.5 Diffusion Proposition and Calculation

4.5.1 Diffusion

The expected band broadening of a sample plug resulting from diffusion may be seen as illustrated in Figure 22. At time zero in case A) the sample plug is introduced into the flow. At time greater than zero $[t_0 + \Delta t_1]$ as shown in case B) the sample plug will diffuse in both direction of the tubing, in positive (x) and in negative (-x) direction based on the concentration gradient. In the

case of C), it is the same situation as in case B), only the time Δt_2 is greater than Δt_1 , therefore the sample distance of diffused sample is greater.

The pictorial illustration in Figure 22 is a strong simplification of the diffusion concept and is meant to give an idea on how the diffusion of a sample plug was pictured.

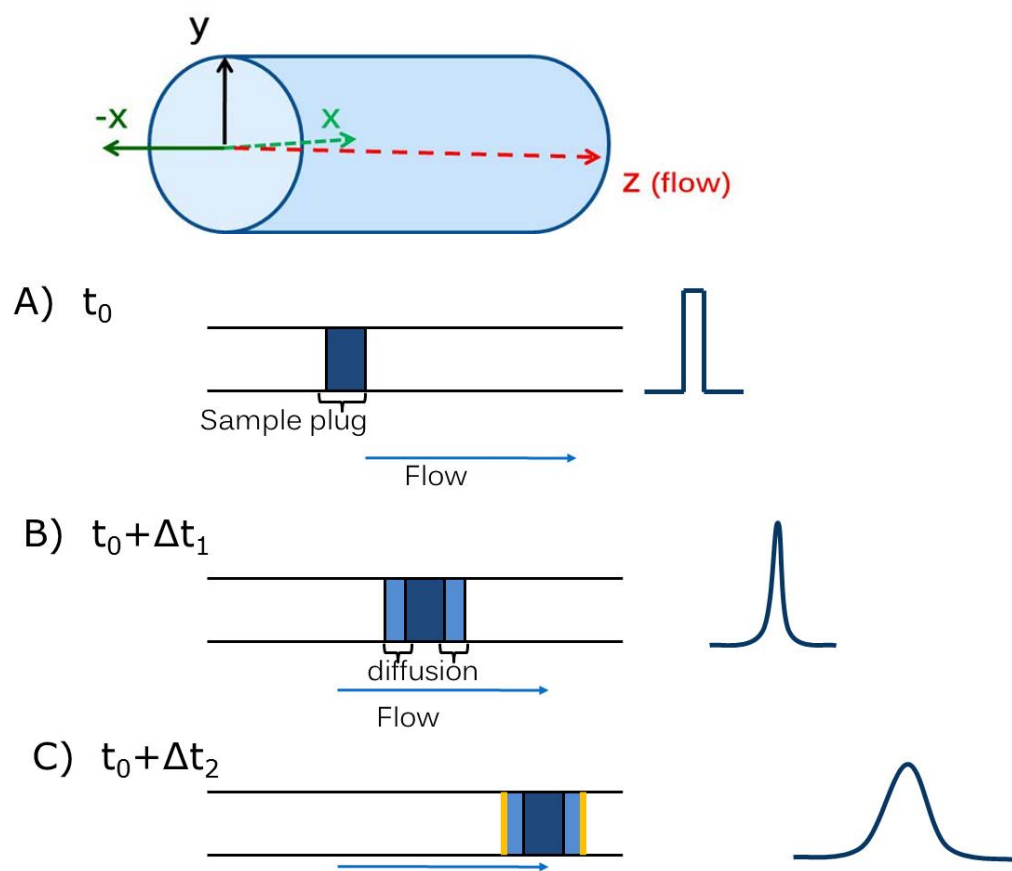


Figure 22: Idea of diffusion of sample plug in PEEK tubing.

At point A) the sample plug is introduced to the tubing. Here we will assume that the plug is the size of the sample volume, in this case 0.5 μl , entering the tubing “undisturbed”. The PEEK tubing used had the dimensions of 914.4 mm length and 0.508 mm ID. The flow rate was at 0.5 ml/min. The sample plug size in length residing in this tubing can be calculated based on the general equation for the volume of a cylinder (see equation 28) and is in this case 2.47 mm long.

Taking the Brownian motion by Einstein into account (see equation 19) the sample plug will experience an increase in length in the axial directions, x and -x but not radial. The time t is the travel time of the sample plug needed to travel through the entire tubing at the given flow rate, for example 0.5 ml/min. Conversion of volumetric flow rate into linear velocity of the flow can be done as follows:

$$v_l = \frac{L_{tub}}{V_{tub} \frac{1}{F}} \quad (44)$$

or

$$v_l = \frac{F}{A} \quad (45)$$

Where v_l is the linear velocity, L_{tub} the length of the entire tubing, V_{tub} the volume of the tubing, and F the volumetric flow rate, A is the cross sectional area of the tubing, and the resulting linear velocity is 246.69 cm/min.

The diffusion coefficient of acetonitrile is $2.13 \cdot 10^{-5} \text{ cm}^2/\text{s}$ [72] and by applying the diffusion equation:

$$x = \sqrt{2D \left(\frac{V_{tub}}{F} \right)} \quad (46)$$

The diffusive distance x and $-x$ can be calculated. The measured peak widths were adjusted to the linear velocity and represented in length by taking the product of the peak width min and the linear velocity. The theoretical predicted value and the measured values are shown in Table 12.

Table 12: Summarization of peak width values from measurements and predictions based on calculation of molecular diffusion. The last row in the table demonstrates the hypothetical value of the sample plug width.

Normalized for tubing volume 0.185 ml (914.4 mm long, ID 0.508 mm)						
F [ml/min]	Measured peak width [min]	Linear velocity [cm/min]	Transition time [min]	Adjusted peak width [cm]	x [cm]	2x + Sample plug [cm]
4.00	0.083	1973.53	0.05	163.21	0.011	0.516
3.00	0.102	1480.15	0.06	150.53	0.013	0.519
2.00	0.143	986.76	0.09	141.40	0.015	0.525
1.00	0.265	493.38	0.19	130.75	0.022	0.537
0.50	0.475	246.69	0.37	117.18	0.031	0.556
0.10	1.357	49.34	1.85	66.94	0.069	0.632
0.05	2.100	24.67	3.70	51.81	0.097	0.688
0.005	7.583	2.47	37.00	18.71	0.308	1.109
0.0025	13.416	1.23	74.00	16.55	0.435	1.364
0.001	34.000	0.49	185.00	16.77	0.688	1.869

The sample plug is treated as a non-deformable cylinder (as pictured in Figure 22) which stays constant while flowing through the tubing. The only change in size is caused by diffusion in the longitudinal direction (x and $-x$). The last column in Table 12 is the maximum possible sample plug size with the assumption that the diffusion amount is identically in x and $-x$ direction ($2x$), therefore adding $2x$ to the length of the sample plug. The data confirms that the band broadening caused by diffusion is insignificant in comparison of the overall band broadening. It actually had an opposite effect than we expected.

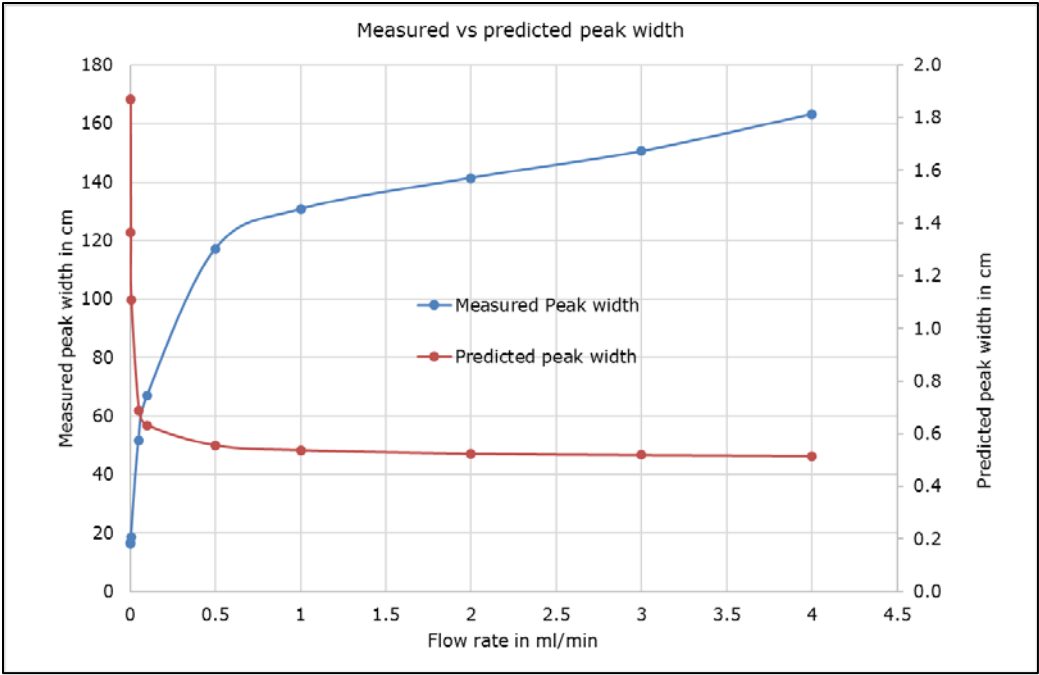


Figure 23: Comparison of measured and predicted peak width, demonstrating that the measured results are the opposite of what was expected.

4.5.2 Flow contribution

As stated before, if the Reynolds number is lower than 2000, there will be a laminar flow in the tubing. The Reynolds number for the different mobile phases and different tubing inner diameters are shown in Table 13. As can be seen in Table 13, for flow rate of 5 ml/min on the tubing with an ID of 0.508 mm, the flow is in the transitional and even in the turbulent flow regime. A steady laminar flow is not present.

In the previous part of this work, the entrance length of the laminar flow profile has been discussed and showed that it was possible to estimate the length needed in order to develop a laminar flow profile (see equation 14) [40,49]. To confirm that the time is sufficient to develop a laminar flow profile, the equation (14) was applied to a set of data with acetonitrile as mobile phase which should represent all other experiments done in the same way. The data table 14 clearly show that the time needed to develop a laminar flow profile is very short in comparison to the dwell time; which is the time the fluid requires to travel the entire length of the tubing. The dwell time and development time are calculated with the linear velocity. It can also be seen that a turbulent flow profile develops much faster than a laminar flow profile. For turbulent flow following equations is used [49]:

$$L_{h_{turbulent}} \approx 4.4 * Re^{\frac{1}{6}} * D \quad (47)$$

Table 13: Reynolds number for different mobile phases, flow rate and tubing sizes.

F ml/min	Reynolds number								
	ID 0.508 mm			ID 0.254 mm			ID 0.178 mm		
	MeCN	MeOH	H2O	MeCN	MeOH	H2O	MeCN	MeOH	H2O
5	4690	3042	2302	2345	1521	1151	1641	1065	806
2	1876	1217	921	938	608	460	657	426	322
1	938	608	460	469	304	230	328	213	161
0.5	469	304	230	234	152	115	164	106	81
0.1	94	61	46	47	30	23	33	21	16
0.05	47	30	23	23	15	12	16	11	8
0.01	9	6	5	5	3	2	3	2	2
0.005	5	3	2	2	2	1	2	1	1
0.001	1	1	0	0	0	0	0	0	0

Table 14: Shows the time needed of the flow to develop a laminar flow profile based on equation (14). The dwell time is the time needed for the fluid to travel the entire length of the capillary.

Tubing ID in mm	Flow rate in ml/min	Reynolds number	Entrance length L _h in cm	Velocity v in cm/min	dwell time d _t in s	time needed to develop entrance length in s
0.508	0.1	94	0.29	49.34	111.20	0.348
	0.5	469	1.43	246.69	22.24	0.348
	1	938	2.86	493.38	11.12	0.348
	2	1876	5.72	986.76	5.56	0.348
	5	4690	14.30	2466.90	2.22	*0.348
0.254	0.1	47	0.07	197.35	27.80	0.022
	0.5	234	0.36	986.76	5.56	0.022
	1	469	0.71	1973.52	2.78	0.022
	2	938	1.43	3947.04	1.39	0.022
	5	2345	3.57	9867.60	0.56	*0.022
0.178	0.1	33	0.04	402.76	13.62	0.005
	0.5	164	0.17	2013.80	2.72	0.005
	1	328	0.35	4027.59	1.36	0.005
	2	657	0.70	8055.19	0.68	0.005
	5	1641	1.75	20137.97	0.27	0.005

* values should not be used, since the Reynolds number for those data indicates that the flow is in the transitional and/or turbulent flow region and therefore will need another equation to solve it. The numbers are 0.022 s and 0.0001 s respectively.

The development of laminar flow profile leads to the longitudinal shift of the liquid layers essentially creating the interface between sample reach zone and pure mobile phase in lateral direction. This causes significant chemical potential gradient leading to the lateral diffusive flux, which will be specified as the rolling effect. The rolling effect is the situation where the sample plug layer on the wall has a velocity equal to zero. The deformation of the plug into a parabolic profile provides two main areas where diffusion takes place. The molecule, which travels in the very center of the tube (horizontal) and the very front of it (vertical), possesses the greatest velocity. At this position, there is an interface between analyte plug and mobile phase. Since the diffusion is mainly directed from higher concentration into lower concentration, this molecule will diffuse outwards (towards the wall) into the lower concentrated layer which has a smaller velocity.

The molecular transfer from inner layers outward is the transfer from smaller volume to the bigger volume, so the concentration gradient is higher than otherwise and thus more favorable than transfer from outer layer to the inner layer as pictured in Figure 24. This leads to the creation of the higher sample concentration in the peripheral layers that have relatively slow velocity Figure 25. This cause overall delay of the peak maxima relative to the average fluid velocity.

On the other hand, the molecule on the wall with the velocity equals to zero will diffuse inward (towards the tubing center) and will therefore penetrate into a layer with greater velocity. This effect which happens simultaneously

(on the back and the front of the parabolic analyte plug) is called rolling effect. The sample plug is driven forwards by this effect. Those situations are illustrated in Figure 26.

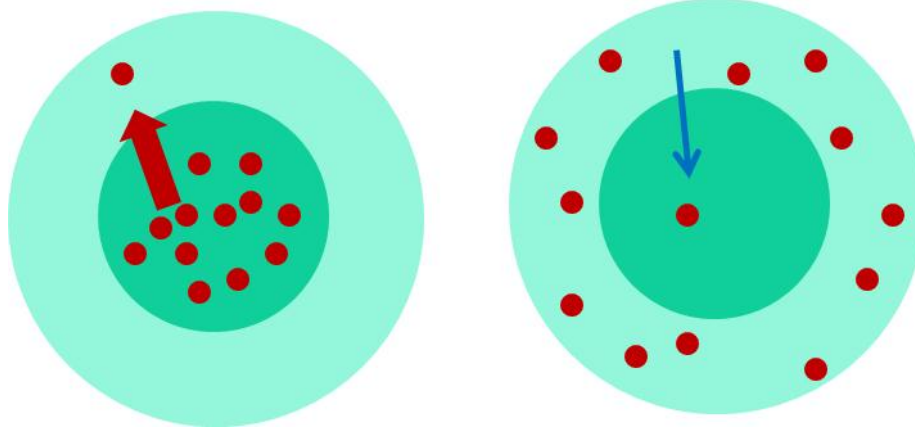


Figure 24: Diffusion from the inner layer outwards is more favorable than the diffusion from the outer layer inwards.

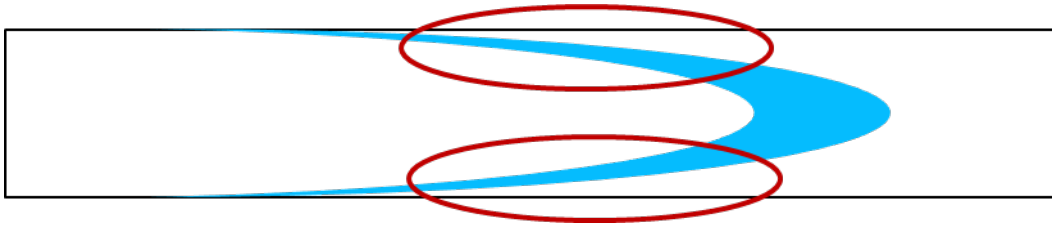


Figure 25: Concentration gradient from the parabolic flow profile towards the tubing wall, where the concentration on the peripheral layer towards the tubing wall is presumed to be higher.

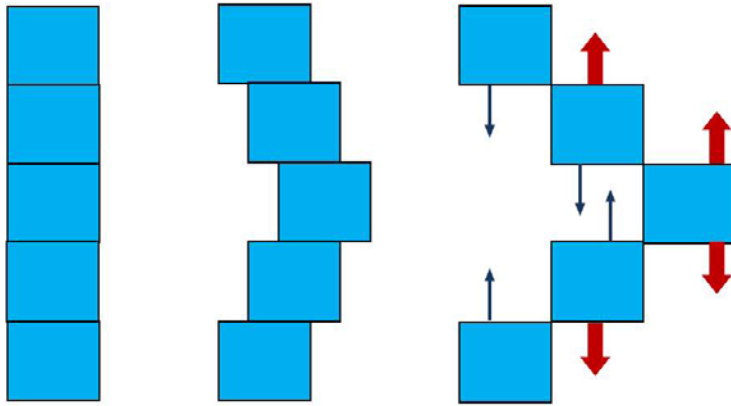


Figure 26: Diffusion direction of the sample plug. The molecules diffuse outward (red arrows) from a higher velocity and concentration into a layer with a lower concentration and slower velocity, whereas the blue arrows demonstrate the direction of the diffusion from the outside layers exhibiting slower velocity into the layer with higher velocity and concentration.

Using the data collected and looking back to Taylor's statement that axial diffusion can be neglected as far as the conditions in equation (35) are satisfied.

$$\frac{4L}{a} \gg \frac{aU}{D} \gg 6.9$$

Table 15 illustrates that all of the experimental value fall under the regime that the conditions are far greater than 6.9. If following that statement, further investigations can be done by neglecting axial diffusion.

Table 15: Calculation based on equation (25) to see if the conditions are greater than 6.9. The data below confirm that to be true. Therefore, axial diffusion in future calculation can be neglected.

F in ml/min	aU/D		
	ID 0.508 mm	ID 0.254 mm	ID 0.178 mm
5	483901	241950	169365
2	193560	96780	67746
1	96780	48390	33873
0.5	48390	24195	16937
0.1	9678	4839	3387
0.05	4839	2420	1694
0.01	968	484	339
0.005	484	242	169
0.001	97	48	34
4L/a	144000	288000	411429

Using the equation proposed from Taylor, the resulting peak width is graphed together against the measured peak width. Previously, the peak width was compared with the molecular diffusion equation. This time the peak width is compared with the Taylor's dispersion coefficient. As illustrated in Figure 27 the dispersion proposed by Taylor does increase at higher flow rate and therefore follows the trend we observed in our experiment. The dispersion coefficient K however is independent from the inner diameter of the tubing. The data also shows that by using the Taylor dispersion coefficient K , the dispersion is strongly underestimated especially at lower flow rate. Additionally, the experimental data show a rather logarithmic tendency whereas the data based on Taylor depict more of a polynomial tendency.

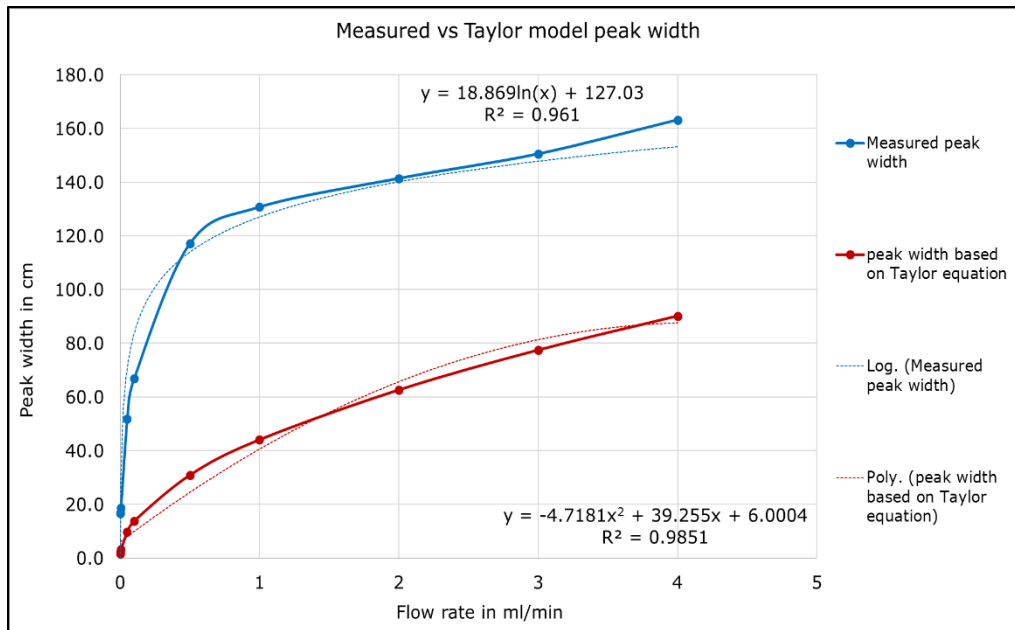


Figure 27: Experimental peak width compared to the Taylor equation for the dispersion coefficient K .

Up to this point it has been established that the diffusion in the sample plug can be neglected based on the experimental data observed as well as model calculations. Additionally, it has been established that nearly all experiments were performed within the region where there is an established laminar flow profile. This leads to the conclusion that the dispersion of the sample plug is caused primarily by the flow profile. The band broadening and the resulting apparent increase of retention volume can be explained by flow profile. The initial sample plug with the assumptive cylindrical shape is "deformed" by the flow within the capillary. This causes the sample plug length to increase significantly with the shift of the concentration towards periphery of the capillary (see Figure 28).

The following illustration (Figure 28) provides a conceptual trend and not an actual value. The hypothesis is, that at v_{avg} the overall concentration of the sample plug is at its highest based on the parabolic flow profile, the following diffusion tendency, and the resulting overall concentration distribution of the sample within the area of the tubing at that particular moment in time. This concentration is noticed by the detector and the following peak maxima is shifted based on the flowrate. This effect is usually not noticeable since the measured retention time is measured in regards on the volumetric flow rate, which is a common practice, but not as liner velocity. By determining the capacity factor $k = (t_r - t_0) / t_0$ the effect of band broadening caused by the different velocity is neglected.

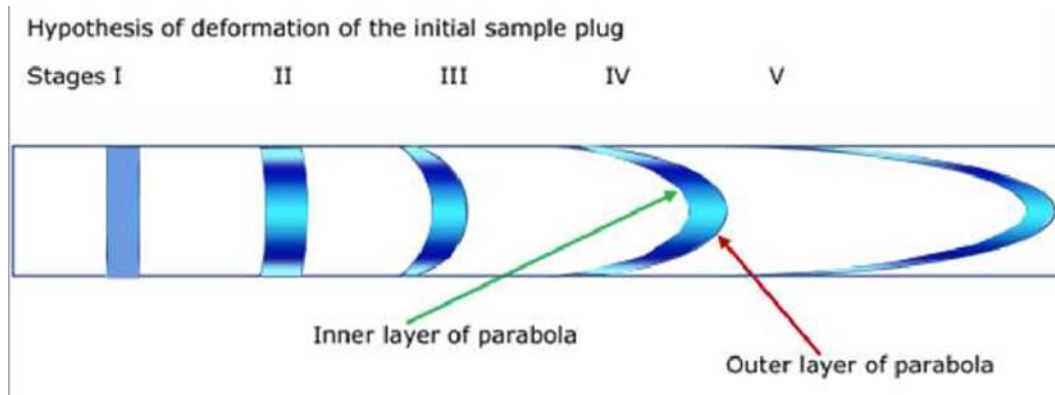


Figure 28: Suggestion of the deformation of the initial sample plug travelling through the capillary

To visualize the flow problem better, the conditions were calculated and plotted in Microsoft Excel. Since the flow profile is of a parabolic nature, it is only natural to use the equation for a parabola [73]:

$$y = ax^2 + bx + c \quad (48)$$

And for the vertex of the parabola:

$$y = a(x - h)^2 + k \quad (49)$$

The presumption was that the x is the distance of the length of the capillary, y is the radius of the capillary and therefore the known vertex is at (0,0) to simplify the calculation. The vertex is actually at $y = \text{radius} = 0$ cm and $x = \text{end of the capillary} = 914.4$ mm. By solving for a with the known point of vertex and with y maximum equals the radius of the tubing and x maximum equals the length of the tubing, the shape of the parabola can be calculated. Additionally, the assumption was made that by calculating two parabolas; one as the "outer layer" and one as the "inner layer", the sample plug profile can be estimated as shown in Figure 28.

It is important to note, that during the modelling of the flow profile, the following assumptions were made:

- The sample is injected into a fully developed laminar flow
- The initial distribution of the sample at time = 0 is uniform over the cross section of the tubing
- Radial diffusion was neglected
- Axial diffusion was neglected
- The density difference between the sample and mobile phase is negligible
- Molecular diffusion coefficient is independent of the sample concentration

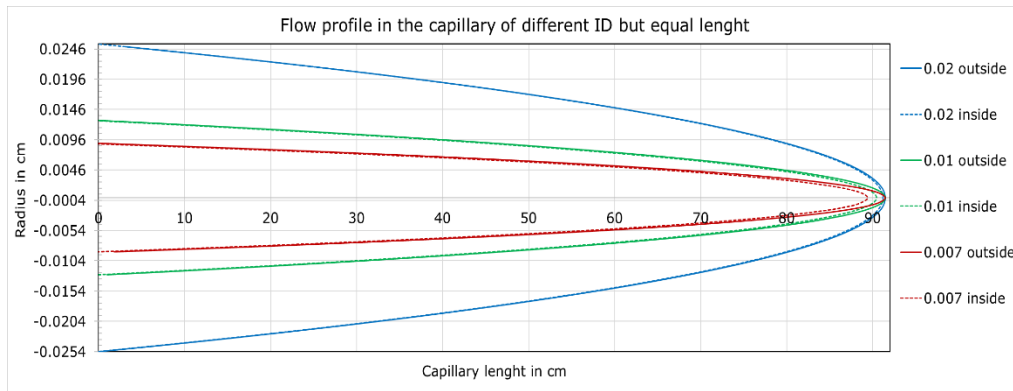


Figure 29: Illustrates the parabolic flow profile of the 3 tubings with different size inner diameters. The limit of the x axis is the limit of the length of the capillary and the limit of the y axis is the limit of the radius of the biggest capillary (ID 0.508 mm).

(Tubing ID 0.02" = 0.508 mm, 0.01" = 0.254 mm and 0.007" = 0.178 mm)

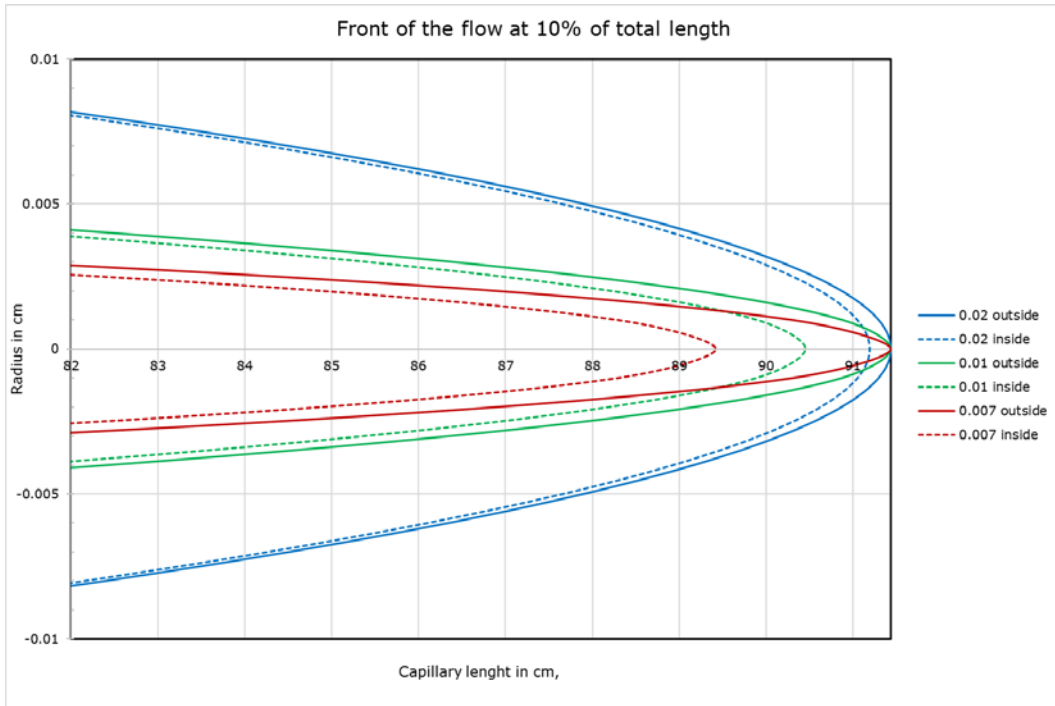


Figure 30: Illustrates the last 10% of the capillary length based on the parabolic flow profile.

(Tubing ID 0.02" = 0.508 mm, 0.01" = 0.254 mm and 0.007" = 0.178 mm)

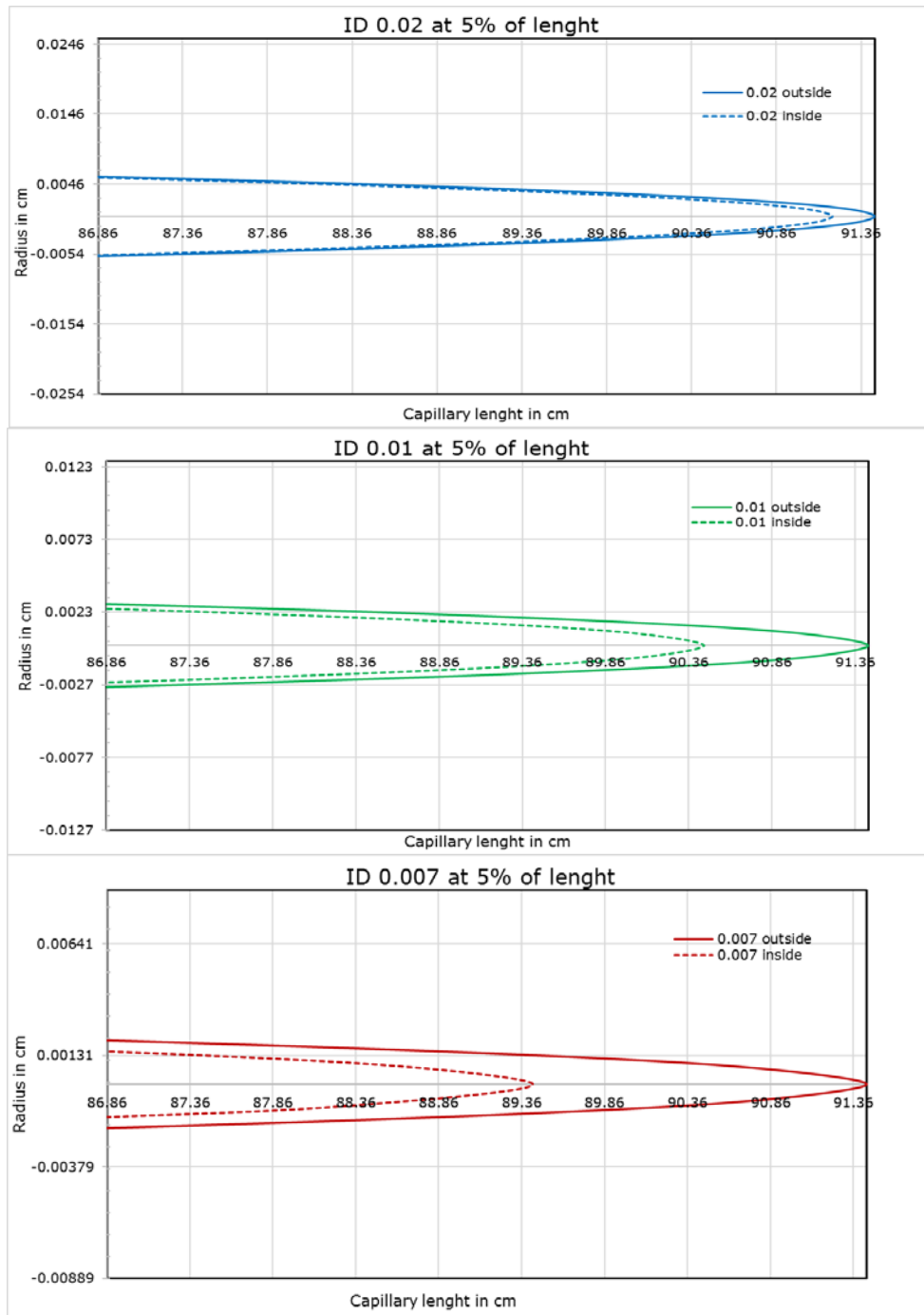


Figure 31: Illustrates the last 5% of the capillary length. The difference in the distance of the outside and inside parabola is increasing by decreasing the capillary ID.

(Tubing ID 0.02" = 0.508 mm, 0.01" = 0.254 mm and 0.007" = 0.178 mm)

Reviewing the results of these experiments, it is clear that the contribution in the apparent increase in retention volume is mostly caused by the flow profile, the dispersion of the sample plug in the longitudinal direction and the additional diffusion between the layers of different concentration and velocities, and finally that the molecular diffusion in and of itself is negligible. Figure 31 shows that the difference between the two parabolas are greatest on the capillary with the smallest inner diameter. This explains why the effect of increasing retention volume is greater on the capillary with smaller inner diameters.

4.6 Model Application

Information gained through these experiments are applicable to building a model for further experiments. Through the previous experiments the average of the apparent increase of retention volume is about 31 μl . This volume itself is not very big, but considering the sample volume of 0.5 μl and comparing it with the column void volume, the 31 μl can make a significant difference in the overall separation of the sample. Assuming the column void volume is about 60 % of the column volume empty (without stationary phase) the following relationship can be seen in Table 16. The smallest column has a dimension of 1.0 x 50 mm which results in a theoretical column void volume of 23.6 μl . This column void volume is actually 24 % smaller

than the extra column volume of 31 μl . Now, if we imagine that we inject a sample mixture of A and B and that those samples are small molecules which are very low retentive or even non-retentive, and that the retention time for molecule B is one and half time longer than that of the compound A, then the following scenario can be drawn as illustrated in Figure 32, Figure 33, and Figure 34.

For average size HPLC columns the 2 components exhibit a good separation, but if the column size were to be decreased to 2.0 x 50 mm, the shift in the peak maxima is noticeable. Two peaks were compared with each other. The first peak (straight line) is a peak profile without having an extra column contribution at all, but the second peak (dotted line) shows the shift in peak caused by the extra column volume. By further decreasing the column dimension, the differences of the two compounds are getting so small that it is possible to mistake compound B with compound A.

Using the information of the flow profile from our experiments with the resulting dispersion of the sample in the flow, it is clear that the sample does not enter the column as a plug with a uniform cross section but with a "narrow" tip cause by the parabolic flow profile. The sample plug diameter will immediately decrease as the travel distance increases. Therefore, the entrance into the HPLC column of the sample plug will be so small, that in the case of a very small and short column, it is conceivable that the sample plug will not be able reach the column wall and the separation process is focused in the center of the column. In a bigger column, the change in diameter from

the exit of the capillary into the entrance of the column is significantly bigger, so the resulting mixing of the fluid caused by the eddy diffusion within the column will give the sample enough time to "mix" within the space. The difference in linear velocity will decrease significantly as the sample enters the column so that the "rest" of the sample will have enough time to "catch-up".

Table 16: Overview of different column dimensions and the resulting ratio of the column void in comparison to the extra column volume of 31 μl .

Column dimension	Volume of cylinder V_c	Theoretical V_{oc} of column ($\sim 60\%$ of V_c)	Ratio $V_{oc} : V_{ecv}$
1.0 x 50 mm	39.3 μl	23.6 μl	5:7
2.0 x 50 mm	157.1 μl	94.2 μl	3:1
3.0 x 50 mm	353.4 μl	212.1 μl	7:1
4.6 x 150 mm	2492.9 μl	1495.7 μl	48:1

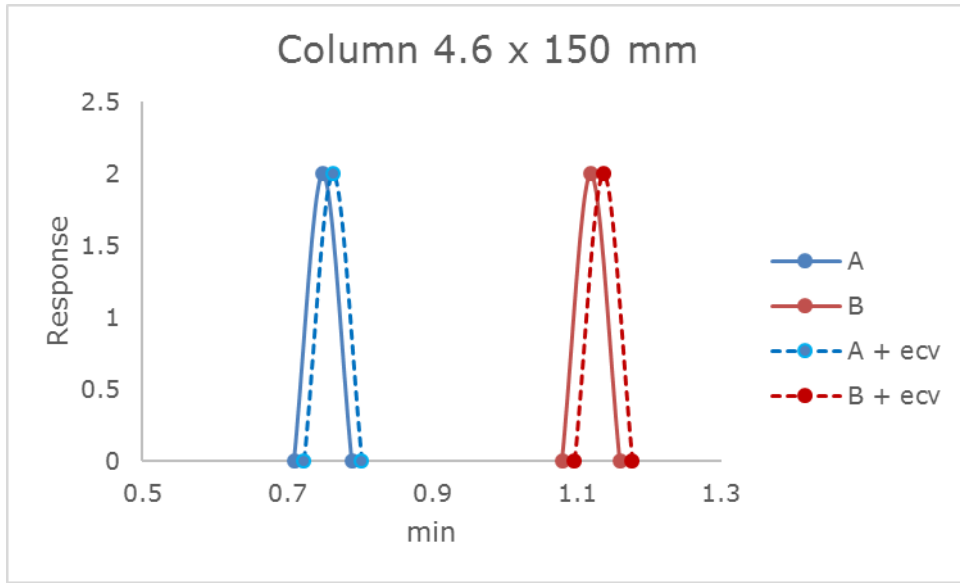


Figure 32: Effect of extra column volume on analyte retention on a column with dimensions of 4.6 x 150 mm.

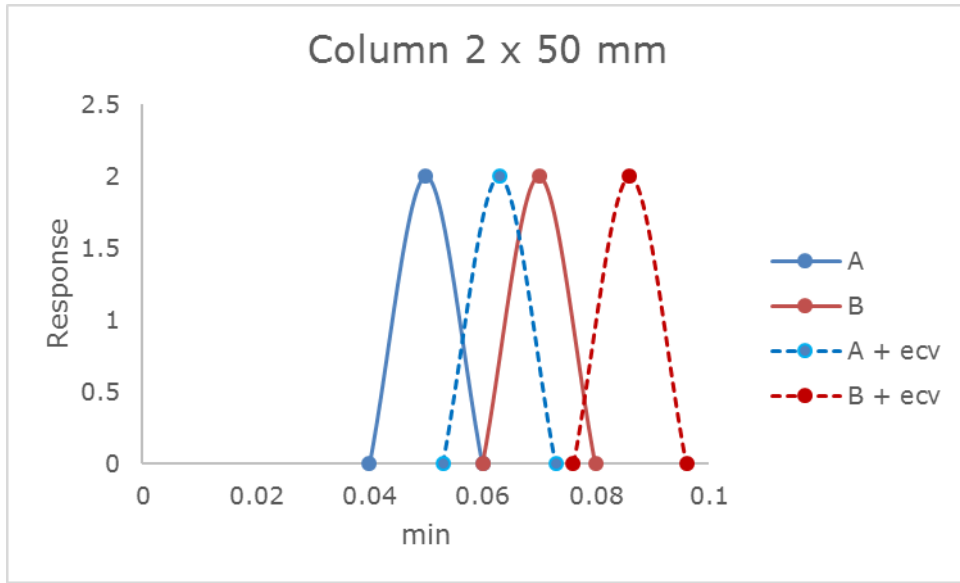


Figure 33: Effect of extra column volume on analyte retention on a column with dimensions of 2 x 50 mm.

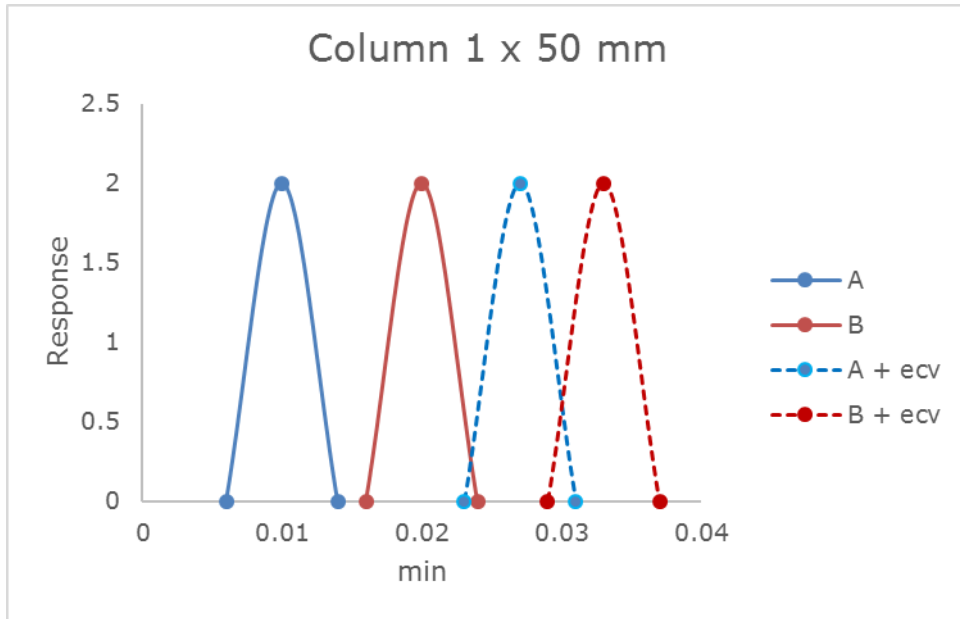


Figure 34: Effect of extra column volume on analyte retention on a column with dimensions of 1 x 50 mm.

5. Conclusions

- I. The apparent increase of retention volume in dependency of the flow rate was found to be caused by the laminar flow profile and the concomitant diffusion of the analyte between the layers of the laminar flow profile. This apparent increase in volume is the result of the overall dispersion of the analyte in the tubing and therefore increases the overall band broadening effect.

- II. This research should provide a better understanding of the process that the sample undergoes during its travel through the connective tubing in a HPLC system. It illustrates the importance of the extra column effect on the overall separation in HPLC. The results have shown, that band broadening, caused by longitudinal diffusion (not longitudinal dispersion), will not affect the separation process and cause a detectable band broadening. The results obtained do not diminish band broadening; however, it will assist in the analysis of the chromatographic data with regard to recognizing the extra column effect impact.

- III. Longitudinal molecular diffusion has been found to have negligible effect with regard to band broadening even in very slow and stop flow experiments. This information can be helpful when considering analyses requiring extremely slow flow, stop flow, or "parking" of a sample in the

loop so that the sample will experience a residence time within the tubing; this situation may be necessary in multidimensional liquid chromatography.

- IV. The extra column effects are of themselves the sum of the diffusion as well as the longitudinal dispersion effects caused by the laminar flow profile. The deformation of the sample plug and the resulting concentration gradients between the laminar layers are favoring the diffusion in the radial as well in the longitudinal direction. This effect will be more visible in situations where it is required to have a greater flow rate in order to decrease the analysis time as is seen in the case of UHPLC; additionally, for decreased column dimensions as is the case with very narrow and short columns, and where the additional tubing length is unavoidable, as is the case in multidimensional and coupled chromatographic systems (LC x LC, LC x GC, LC x LC x MS).

- V. For specific and different instrumentation, the effect of the apparent increase of the extra column volume is of interest when considering method transfers between HPLC systems since each system will contain its unique extra column volume and potentially different tubing inner diameters. This may have greatest effect with the method transfer from HPLC systems to UHPLC systems. This extra column contribution can have a significant variable which needs to be considered.

- VI. For the consideration of columns used for HPLC and UHPLC, the extra column effects, which is clearly visible in open capillaries, should also be observable for microcolumns packed with nonporous particles. However, in the case of porous media with interconnected network, this effect may likely be alleviated. The experiments conducted clearly demonstrate that the increase of the theoretical plate height with the decrease of mobile phase linear velocity, which is usually attributed to the effect of longitudinal diffusion, is actually not solely the diffusion effect, but rather the effect of the difference between the interparticle flow and flow inside the pores and diffusive mass transfer between them. This information could be usable for explanation of how the retention factor and peak resolution can be affected in early co-eluting components for different columns and LC systems. Knowing the analyte concentration behavior in the mobile phase can prove useful in the future understanding of the separation process. This can help to provide deeper perspective and help distinguish the multiple effects which are happening at the same time and ultimately contributing to the band broadening within the separation. Another contributing factor is the shape of the parabolic flow profile. In the case of very narrow and short columns, it is conceivable that as the narrow parabolic flow profile enters the column, it will exit the column before the flow could reach the wall of the column. This will cause a non-uniform dispersion of the analyte within the column.
- VII. Therefore, it can be concluded, that the molecular longitudinal diffusion can be neglected in the data evaluation. The longitudinal dispersion

caused by the laminar flow, with its resulting axial and longitudinal diffusion, can cause a considerably noticeable effect which should be taken into consideration in future analyses and for method development and method transfer between laboratories. Additionally, when considering the extra column effect the element of flow rate should be considered since the apparent increase of retention volume revealed the dependency on the flow rate.

6. References

- (1) Kazakevich, Y. V.; Lobrutto, R. *HPLC for Pharmaceutical Scientists*; Kazakevich, Y. V., Lobrutto, R., Eds.; John Wiley & Sons, Inc.: Hoboken, New Jersey, 2007.
- (2) Unger, K.; Ditz, R.; Machtejevas, E.; Skudas, R. *Angew. Chemie* **2010**, *122* (13), 2350–2363.
- (3) Horvath, C. G.; Preiss, B. A.; Lipsky, S. R. *Anal. Chem.* **1967**, *39* (12), 1422–1428.
- (4) Majors, R. E. *LCGC North Am.* **2015**, *33* (11), 818–840.
- (5) Núñez, O.; Gallart-Ayala, H.; Martins, C. P. B.; Lucci, P.; Busquets, R. *J. Chromatogr. B* **2013**, *927*, 3–21.
- (6) Nazario, C. E. D.; Silva, M. R.; Franco, M. S.; Lanças, F. M. J. *Chromatogr. A* **2015**, *1421*, 18–37.
- (7) Ishihama, Y. *J. Chromatogr. A* **2005**, *1067* (1–2), 73–83.
- (8) Xu, A. Q. *Ultra-High Performance Liquid Chromatography and Its Applications*; John Wiley & Sons, Inc.: Hoboken, New Jersey, 2013.
- (9) Nováková, L.; Vlčková, H. *Anal. Chim. Acta* **2009**, *656* (1–2), 8–35.
- (10) Jacoby, M. *Chem. Engermeering News* **2008**, *86* (17), 17–23.
- (11) Fountain, K. J.; Neue, U. D.; Grumbach, E. S.; Diehl, D. M. *J. Chromatogr. A* **2009**, *1216* (32), 5979–5988.
- (12) Fekete, S.; Fekete, J. *J. Chromatogr. A* **2011**, *1218* (31), 5286–5291.
- (13) Gritti, F.; Guiochon, G. *J. Chromatogr. A* **2010**, *1217* (49), 7677–7689.
- (14) Prüss, A.; Kempter, C.; Gysler, J.; Jira, T. *J. Chromatogr. A* **2003**, *1016* (2), 129–141.

- (15) Knox, J. H.; Kaliszan, R. *J. Chromatogr.* **1985**, *349*, 211–234.
- (16) Gritti, F.; Kazakevich, Y.; Guiochon, G. *J. Chromatogr. A* **2007**, *1161* (1–2), 157–169.
- (17) Rimmer, C. A.; Simmons, C. R.; Dorsey, J. G. *J. Chromatogr. A* **2002**, *965* (1–2), 219–232.
- (18) Sajonz, P. *J. Chromatogr. A* **2004**, *1050* (2), 129–135.
- (19) Gritti, F.; Guiochon, G. *J. Chromatogr. A* **2005**, *1097* (1–2), 98–115.
- (20) Neue, U. D. *HPLC Columns Theory, Technology, and Practice*; Wiley-VCH, Inc.: New York, 1997.
- (21) Denney, R. C. *A Dictionary of Chromatography*, 2nd ed.; Wiley Interscience: New York, 1982.
- (22) Giddings, J. C. *Unified Separation Science*; John Wiley & Sons, Inc.: New York, 1991.
- (23) Rathore, A. S.; Horváth, C. *J. Chromatogr. A* **1996**, *743* (2), 231–246.
- (24) Schure, M. R.; Maier, R. S. *J. Chromatogr. A* **2006**, *1126* (1–2), 58–69.
- (25) Fekete, S.; Ganzler, K.; Fekete, J. *J. Pharm. Biomed. Anal.* **2011**, *54* (3), 482–490.
- (26) Gritti, F.; Felinger, A.; Guiochon, G. *J. Chromatogr. A* **2006**, *1136* (1), 57–72.
- (27) Giddings, J. C. *Dynamics of Chromatography Principles and Theory*, 1st ed.; Giddings, J. C., Keller, R. A., Eds.; Marcel Dekker, Inc.: New York, 1965.
- (28) Kirkup, L.; Foot, M.; Mulholland, M. *J. Chromatogr. A* **2004**, *1030* (1–2), 25–31.
- (29) Knox, J. H. *J. Chromatogr. A* **2002**, *960* (1–2), 7–18.

- (30) Gritti, F.; Guiochon, G. *J. Chromatogr. A* **2011**, *1218* (29), 4632–4648.
- (31) Snyder, L. R. In *High-Performance Liquid Chromatography*; Horvath, C., Ed.; Academic Press: New York, 1980; pp 207–316.
- (32) Hughes, W. F.; Brighton, J. A. Gilson, B., Pelton, P., Walker, M. B., Eds.; McGraw-Hill: New York, 1999; p 369.
- (33) Truckenbrodt, E. *Fluidmechanik Band 1, Vierte.*; Springer: Berlin, 1996.
- (34) Niewiadomski, C.; Paraschivoiu, M.; Sullivan, P. *Int. J. Numer. Methods Fluids* **2006**, *51* (8), 849–879.
- (35) Hof, B.; Westerweel, J.; Schneider, T. M.; Eckhardt, B. *Nature* **2006**, *443* (7107), 59–62.
- (36) Harada, M.; Kido, T.; Masudo, T.; Okada, T. *Anal. Sci.* **2005**, *21* (5), 491–496.
- (37) Orlandi, P. *Phys. Fluids* **2008**, *20* (10), 1–13.
- (38) Mathieu, J.; Scott, J. *An Introduction to Turbulent Flow*; Cambridge University Press: New York, 2000.
- (39) Avila, K.; Moxey, D.; de Lozar, A.; Avila, M.; Barkley, D.; Hof, B. *Science* (80-.). **2011**, *333* (6039), 192–196.
- (40) Cengel, Y.; Cimbala, J. *Fluid Mechanics: Fundamentals and Applications*; 2014.
- (41) Suter, S. P.; Skalak, R. *Annu. Rev. Fluid Mech.* **1993**, *25* (1), 1–20.
- (42) Richardson, S. M. Poiseuille Flow
<http://www.thermopedia.com/content/1042/> (accessed Feb 8, 2017).
- (43) Kaiser, T. J.; Thompson, J. W.; Mellors, J. S.; Jorgenson, J. W. *Anal. Chem.* **2009**, *81* (8), 2860–2868.
- (44) Fani, A.; Camarri, S.; Salvetti, M. V. *Phys. Fluids* **2012**, *24* (8), 1–24.

- (45) Barth, W. L.; Carey, G. F. *Online* **2007**, No. January, 1313–1325.
- (46) Fargie, D.; Martin, B. W. *Proc. R. Soc. A Math. Phys. Eng. Sci.* **1971**, 321 (1547), 461–476.
- (47) Vrentas, J. *Chem. Eng. Sci.* **2000**, 55 (4), 849–855.
- (48) *Encyclopedia of Agricultural, Food, and Biological Engineering*; Heldmann, D. R., Ed.; Taylor & Francis, 2003.
- (49) Tongpun, P.; Bumrungthaichaichan, E.; Wattananusorn, S. *Songklanakarin J. Sci. Technol.* **2014**, 36 (4), 471–475.
- (50) Bansal, R. K. *Fluid Mechanics*.
- (51) Holland, F. A.; Bragg, R. *Fluid flow for chemical engineers*; Butterworth-Heinemann, 1995.
- (52) Shao, X.; Yu, Z.; Sun, B. *Phys. Fluids* **2008**, 20 (10), 1–12.
- (53) Wentzell, P. D.; Bowdridge, M. R.; Taylor, E. L.; MacDonald, C. *Anal. Chim. Acta* **1993**, 278 (2), 293–306.
- (54) Cussler, E. L. *Diffusion Mass Transfer in Fluid Systems*, Second.; Cambridge University Press: New York, 2008.
- (55) Ursell, T. S. *The Diffusion Equation: A Multi- dimensional Tutorial*; 2013.
- (56) Holley, E. R. Springer Netherlands, 1996; pp 111–151.
- (57) Philibert, J. *English* **2005**, 2, 1–10.
- (58) Einstein, A. *Ann. Phys.* **1905**, 322 (8), 549–560.
- (59) Okada, T.; Harada, M.; Kido, T. *Anal. Chem.* **2005**, 77 (18), 6041–6046.
- (60) Golay, M. J. E. *Journal of Chromatography A*. December 30, 1979, pp 341–351.

- (61) Ekambara, K. *Chem. Eng. Sci.* **2004**, *59* (18), 3929–3944.
- (62) Farooq, S. *Chem. Eng. Sci.* **2003**, *58* (1), 71–80.
- (63) Shankar, A.; Lenhoff, A. M. *Journal of Chromatography A*. September 6, 1991, pp 235–248.
- (64) Tseng, C. M.; Besant, R. W. *Proc. R. Soc. A Math. Phys. Eng. Sci.* **1970**, *317* (1528), 91–99.
- (65) Andersson, B.; Berglin, T. *Proc. R. Soc. A Math. Phys. Eng. Sci.* **1981**, *377* (1770), 251–268.
- (66) Taylor, G. *Proceedings of the Royal Society A: Mathematical, Physical and Engineering Sciences*. 1953, pp 186–203.
- (67) Taylor, G. *Proc. R. Soc. A Math. Phys. Eng. Sci.* **1954**, *225* (1163), 473–477.
- (68) Aris, R. *Proc. R. Soc. A Math. Phys. Eng. Sci.* **1956**, *235* (1200), 67–77.
- (69) Bailey, H. R.; Gogarty, W. B. *Proc. R. Soc. A Math. Phys. Eng. Sci.* **1962**, *269* (1338), 352–367.
- (70) Atwood, J. G.; Golay, M. J. E. *Journal of Chromatography A*. November 20, 1981, pp 97–122.
- (71) Golay, M. J. E.; Atwood, J. G. *Journal of Chromatography A*. December 30, 1979, pp 353–370.
- (72) Dortmund Data Bank DDBST GmbH <http://www.ddbst.com/> (accessed Feb 20, 2017).
- (73) Meidenbauer, J. *Grosser Ratgeber Mathematik*; Buch und Zeit Verlagsgesellschaft mbH: Koeln, 1997.